Heteronuclear Iron–Ruthenium Complexes Containing Bridging Allenyl and Allenylcarbonyl Ligands

Chris E. Shuchart and Andrew Wojcicki*

Department of Chemistry, The Ohio State University, Columbus, Ohio 43210

Mario Calligaris,† Paolo Faleschini, and Giorgio Nardin

Dipartimento di Scienze Chimiche, Università di Trieste, 34127 Trieste, Italy

Received January 10, 1994®

Reactions of $Cp(CO)_2RuCH_2C{\equiv}CPh$ (**1**) with $Fe_2(CO)_9$ yield one or more of the products $(CO)_3Fe(\mu\text{-}\eta^3{:}\eta^2\text{-}C(O)C(Ph){=}C{=}CH_2)Ru(CO)Cp$ (**2**), $(CO)_3Fe(\mu_2\text{-}CO)RuCp(\mu_2\text{-}CO)Fe(CO)_3(\mu_3\text{-}\eta^1\text{-}CCH{=}CHPh)$ (**3**), $(CO)_3FeRu(CO)CpFe(CO)_3(\mu_3\text{-}\eta^1{:}\eta^1{:}\eta^3\text{-}CCHCHPh)$ (**4**), $(CO)_3FeFe(CO)_3Ru(CO)Cp(\mu_3\text{-}\eta^1{:}\eta^2{:}\eta^2\text{-}C(Ph){=}C{=}CH_2)$ (**5**), and $(CO)_3FeFe(CO)_3Ru(CO)Cp(\mu_3\text{-}\eta^1{:}\eta^2{:}\eta^2\text{-}CH{=}C{=}CHPh)$ (**6**), depending on solvent, relative amounts of the reactants, and reaction time and temperature. The novel binuclear metal μ-allenylcarbonyl complex **2** is best prepared in THF at 0 °C, whereas the "capped" trinuclear metal clusters **3** and **4** are obtained, along with **2**, in diethyl ether at reflux. The trinuclear metal $\mu_3\text{-}\eta^1{:}\eta^2{:}\eta^2$-allenyl products **5** and **6** result from the reaction of **1** with a large excess of $Fe_2(CO)_9$ in hexane at reflux. In the formation of **3**, **4**, and **6**, a methylene hydrogen shift occurs within the C_3H_2Ph ligand. Reaction of **1** with $Ru_3(CO)_{12}$ in hexane at reflux affords $(CO)_3RuRu(CO)_3Ru(CO)Cp(\mu_3\text{-}\eta^1{:}\eta^2{:}\eta^2\text{-}C(Ph){=}C{=}CH_2)$ (**7**), which is structurally analogous to **5**. Complex **2** undergoes monosubstitution at iron with each of PPh_3 and $Ph_2PCH_2PPh_2$ (dppm) at room temperature to yield **8** and **9**, respectively. Thermolysis of $(\eta^1\text{-dppm})(CO)_2Fe(\mu\text{-}\eta^3{:}\eta^2\text{-}C(O)C(Ph){=}C{=}CH_2)Ru(CO)Cp$ (**9**) affords disubstituted, dppm-bridged $(CO)_2Fe(\mu\text{-}\eta^3{:}\eta^2\text{-}C(O)C(Ph){=}C{=}CH_2)(\mu\text{-dppm})RuCp$ (**10**). Reaction of **5** with PPh_3 in hexane at reflux furnishes a monosubstitution product with Fe—PPh_3 bonding. All complexes were characterized by a combination of elemental analysis, mass spectrometry, and IR and ^1H, ^{13}C, and ^{31}P NMR spectroscopy. The structures of **2**, **5**, and **6** were determined by X-ray diffraction analysis. **2**: monoclinic, $P2_1/c$, a = 7.037(5) Å, b = 17.20(1) Å, c = 29.69(2) Å, β = 95.58(5)°, Z = 8, R = 0.065, R_w = 0.074; **5**: monoclinic, $P2_1/c$, a = 8.068(3) Å, b = 15.333(4) Å, c = 16.849(3) Å, β = 95.11(1)°, Z = 4, R = 0.037, R_w = 0.042; **6**: monoclinic, $P2_1/c$, a = 8.999(4) Å, b = 12.914(6) Å, c = 36.15(1) Å, β = 93.46(2)°, Z = 8, R = 0.057, R_w = 0.075.

Introduction

Reactions of transition-metal propargyl complexes with iron and ruthenium carbonyls serve as convenient synthetic methods for binuclear and trinuclear metal compounds with bridging hydrocarbyl ligands.[1-5] Molybdenum and tungsten propargyl complexes of the type $Cp(CO)_3MCH_2C{\equiv}CR$ (R = alkyl, aryl) afford heterobinuclear and heterotrinuclear μ-allenyl products as illustrated in eq 1 for $Fe_2(CO)_9$.[1,6] In contrast, the iron propargyl $Cp(CO)_2FeCH_2C{\equiv}CPh$ reacts with $Fe_2(CO)_9$ to give a binuclear iron complex that does not possess a metal–metal bond

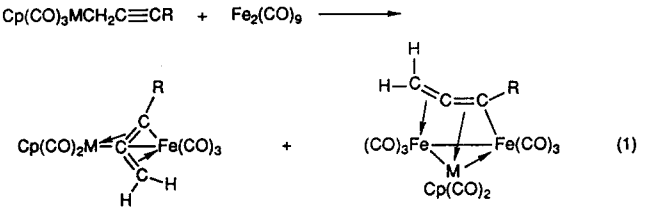

(1)

(eq 2),[2,3] and the isoelectronic chromium propargyl Cp-

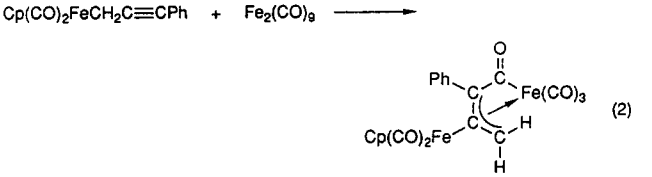

(2)

$(NO)_2CrCH_2C{\equiv}CPh$ reacts with $Fe_2(CO)_9$ under comparable conditions to yield $(CO)_3Fe(\mu\text{-}\eta^3{:}\eta^2\text{-}C(Ph){=}C{=}CH_2)Fe(CO)_2NO$ and $CpCr(CO)_2NO$.[3] Furthermore, reactions of the η^1-vinylpropargyl complex $(CO)_5MnCH_2C{\equiv}CCH{=}CH_2$ with $Fe_2(CO)_9$ proceed to binuclear and trinuclear mixed-metal compounds that show no Fe–Mn bonding.[4a] Thus, whereas the second- and third-row transition-metal propargyls have furnished products containing bonds between metal atoms of the two reactants,

† To whom inquiries concerning X-ray crystallographic work should be addressed.

® Abstract published in *Advance ACS Abstracts,* April 15, 1994.

(1) (a) Young, G. H.; Wojcicki, A.; Calligaris, M.; Nardin, G.; Bresciani-Pahor, N. *J. Am. Chem. Soc.* **1989,** *111,* 6890. (b) Young, G. H.; Raphael, M. V.; Wojcicki, A.; Calligaris, M.; Nardin, G.; Bresciani-Pahor, N. *Organometallics* **1991,** *10,* 1934.

(2) Shuchart, C. E.; Young, G. H.; Wojcicki, A.; Calligaris, M.; Nardin, G. *Organometallics* **1990,** *9,* 2417.

(3) Young, G. H.; Willis, R. R.; Wojcicki, A.; Calligaris, M.; Faleschini, P. *Organometallics* **1992,** *11,* 154.

(4) (a) Cheng, M.-H.; Lee, G.-H.; Peng, S.-M.; Liu, R.-S. *Organometallics* **1991,** *10,* 3600. (b) Cheng, M.-H.; Shu, H.-G.; Lee, G.-H.; Peng, S.-M.; Liu, R.-S. *Organometallics* **1993,** *12,* 108.

(5) (a) Wojcicki, A.; Shuchart, C. E. *Coord. Chem. Rev.* **1990,** *105,* 35. (b) Wojcicki, A. *J. Cluster Sci.* **1993,** *4,* 59.

(6) However, reactions of $Cp(CO)_3WCH_2C{\equiv}CCH{=}CH_2$ and $Cp(CO)_3WCH_2C{\equiv}CCH_2W(CO)_3Cp$ with $Fe_2(CO)_9$ are more complex than those of the corresponding tungsten alkyl- and arylpropargyl complexes.[4]

0276-7333/94/2313-1999$04.50/0

the first-series transition-metal propargyls have afforded products without such metal–metal bonds. Possibly, this difference in behavior arises because the heavier transition metals generally form stronger metal–metal bonds than the transition metals of the first series.[7]

In order to test further these generalities, we have conducted a study of reactions of the ruthenium propargyl complex $Cp(CO)_2RuCH_2C{\equiv}CPh$ (1) with iron and ruthenium carbonyls. It was of particular interest to compare and contrast the behavior of 1 with that of the congeneric $Cp(CO)_2FeCH_2C{\equiv}CPh$ and the second- and third-series transition-metal propargyls $Cp(CO)_3MCH_2C{\equiv}CR$ (M = Mo, W). Ruthenium compounds generally are more stable than their iron counterparts, and ruthenium tends to form clusters more readily than does iron.[8,9] Moreover, many ruthenium-containing compounds are catalytically active.[10]

In this paper we report on the reactions of 1 with $Fe_2(CO)_9$ and $Ru_3(CO)_{12}$ and on the structure and reaction chemistry of binuclear and trinuclear mixed-metal products. The reaction of 1 with $Fe_2(CO)_9$ was found to be more complex than the corresponding reactions of both $Cp(CO)_2FeCH_2C{\equiv}CPh$ and $Cp(CO)_3MCH_2C{\equiv}CR$ (M = Mo, W): it furnishes, in addition to trinuclear metal μ-η^1:η^2:η^2-allenyl complexes, trinuclear metal μ_3-alkylidyne products and a novel binuclear μ-η^3:η^2-allenylcarbonyl product. For the first time, a methylene hydrogen shift was found to occur within the C_3H_2R ligand in the reactions of the propargyl complexes with metal carbonyls. Parts of this study were reported earlier in a communication.[2]

Experimental Section

General Procedures and Measurements. All reactions and manipulations of air-sensitive compounds were carried out under an atmosphere of Ar by using standard procedures.[11] Elemental analyses were performed by M-H-W Laboratories, Phoenix, AZ. Melting points were measured on a Thomas-Hoover melting point apparatus and are uncorrected. Infrared, NMR (^1H, ^{13}C, and ^{31}P), and mass spectra (FAB) were obtained as previously described.[1,3]

Materials. All solvents were purified by distillation under an Ar atmosphere prior to use. Hexane and diethyl ether were distilled from Na/K alloy, THF and benzene were distilled from potassium benzophenone ketyl, and CH_2Cl_2 was distilled from CaH_2.

Reagents were obtained from various commercial sources and used as received, except as noted below. Bis(diphenylphosphino)methane (dppm) was recrystallized from ethanol, and trimethylamine *N*-oxide was sublimed from the dihydrate. Literature procedures were used to synthesize $Cp(CO)_2RuCH_2C{\equiv}CPh$,[12] $Fe_2(CO)_9$,[13] and $Ru_3(CO)_{12}$.[14]

Preparation of $(CO)_3Fe(\mu$-η^3:η^2-C(O)C(Ph)=C=CH$_2$)Ru(CO)Cp (2). A yellow solution of $Cp(CO)_2RuCH_2C{\equiv}CPh$ (1; 1.25 g, 3.7 mmol) in THF (150 mL) at 0 °C was treated with solid $Fe_2(CO)_9$ (2.7 g, 7.4 mmol). The resulting suspension was stirred at 0 °C for 24 h, over which time the solution darkened. Solvent was removed in vacuo, and the brown residue was dissolved in a minimum amount of CH_2Cl_2. An equal volume of alumina (6% H_2O) was introduced, and the solvent was evaporated under reduced pressure. The residue was added to the top of a column of alumina (2 × 25 cm) in hexane. Elution with 6–8% (v/v) diethyl ether in hexane yielded a bright yellow band, which was removed from the column. Evaporation of the solvent afforded **2** as an orange solid (0.55 g, 31% yield): dec pt 104 °C; IR (cyclohexane) ν(CO) 2041 (s), 1996 (s), 1975 (s), 1968 (sh), 1776 (sh), 1761, (w-m) cm^{-1}; ^1H NMR ($CDCl_3$) δ 7.81–7.77, 7.44–7.31 (2 m, Ph), 5.00 (s, Cp), 4.07, 3.69 (2 d, ^2J = 6.0 Hz, CH_2); $^{13}C\{^1H\}$ NMR ($CDCl_3$, 220 K) δ 221.7 (s, C=O), 214.3, 210.6, 204.7 (3 s, Fe-CO's), 201.5 (s, Ru—CO), 186.3 (s, =C=), 133.8 (s, ipso C of Ph), 129.1, 128.3, 127.1 (3 s, other C's of Ph), 87.0 (s, Cp), 46.3 (s, =*C*—Ph), 15.3 (s, CH_2); MS (FAB) ^{102}Ru isotope *m/z* 478 (M^+), 450 (M^+ – CO), 422 (M^+ – 2CO), 394 (M^+ – 3CO), 366 (M^+ – 4CO), 338 (M^+ – 5CO), 282 ($CpRuC_9H_7^+$). Anal. Calcd for $C_{19}H_{12}FeO_5Ru$: C, 47.82; H, 2.53. Found: C, 48.16; H, 2.62.

Reaction of $Cp(CO)_2RuCH_2C{\equiv}CPh$ (1) with $Fe_2(CO)_9$ in Diethyl Ether at Reflux. To a solution of 1 (1.25 g, 3.7 mmol) in diethyl ether (150 mL) was added with stirring $Fe_2(CO)_9$ (2.7 g, 7.4 mmol), and the resulting suspension was kept at reflux for 20 min. The mixture turned dark brown as the reaction, monitored by ^1H NMR spectroscopy, reached completion. Solvent was removed in vacuo, and the residue was dissolved in a minimum amount of CH_2Cl_2. The resulting solution was treated with an equal volume of alumina (6% H_2O), CH_2Cl_2 was evaporated under reduced pressure, and the residue was added to the top of a column of alumina (2 × 25 cm) packed in hexane. Elution with 6–8% diethyl ether in hexane gave a yellow-orange band, which was collected and freed of solvent to yield $(CO)_3Fe(\mu$-η^3:η^2-C(O)C(Ph)=C=CH$_2$)Ru(CO)Cp (2; 0.32 g, 18%). Continued elution, now with 15% (v/v) diethyl ether in hexane, removed a brown band, from which a dark brown solid, $(CO)_3Fe(\mu_2$-CO)RuCp(μ_2-CO)Fe(CO)$_3(\mu_3$-η^1-CCH=CHPh) (**3**), was obtained (0.27 g, 12% yield) after evaporation of the solvent: mp >200 °C; IR (hexane) ν(CO) 2055 (s), 2022 (vs), 2012 (s), 1983 (m), 1973 (m), 1876 (w-m), 1839 (m) cm^{-1}; ^1H NMR ($CDCl_3$) δ 9.18 (d, ^3J = 15.2 Hz, =CH), 7.65–7.62, 7.36–7.30 (2 m, Ph), 7.12 (d, ^3J = 15.2 Hz, =CH), 5.80 (s, Cp). Anal. Calcd for $C_{22}H_{12}Fe_2O_8Ru$: C, 42.79; H, 1.94. Found: C, 43.25; H, 2.03. Elution with diethyl ether gave a dark green band, which was collected and freed of solvent to afford a greenish brown solid, characterized as $(CO)_3FeRu(CO)CpFe(CO)_3(\mu_3$-$\eta^1$:$\eta^1$:$\eta^3$-CCHCHPh) (**4**). After washing with hexane, 4 was obtained in 6% yield (0.14 g): IR (CH_2Cl_2) ν(CO) 2048 (s), 2017 (s), 1998 (vs), 1967 (s) cm^{-1}; ^1H NMR ($CDCl_3$) δ 7.42–7.21 (m, Ph), 6.27 (d, ^3J = 8.6 Hz, CH), 5.73 (s, Cp), 3.81 (d, ^3J = 8.6 Hz, CH); MS (FAB) ^{102}Ru isotope *m/z* 589 (M^+ – CO – 1), then consecutive loss of other CO's.

Reaction of $Cp(CO)_2RuCH_2C{\equiv}CPh$ (1) with $Fe_2(CO)_9$ in Hexane at Reflux. A solution of 1 (1.25 g, 3.7 mmol) in hexane (150 mL) was treated with a large excess of solid $Fe_2(CO)_9$ (8.1 g, 22 mmol), and the resulting suspension was kept at reflux for 10 min. The reaction mixture was then worked up similarly to that of the preceding synthesis in diethyl ether solvent. Chromatography on alumina (6% H_2O) with 2–5% (v/v) diethyl ether in hexane as eluent afforded two bands. Solvent removal from the first, olive green band yielded a green-black solid, $(CO)_3FeFe(CO)_3Ru(CO)Cp(\mu_3$-$\eta^1$:$\eta^2$:$\eta^2$-C(Ph)=C=CH$_2$ (**5**; 0.43 g, 18%): mp 144–147 °C; IR (Et_2O) ν(CO) 2064 (sh), 2049 (s), 2011 (vs), 1981 (vs), 1964 (sh), 1923 (w-m) cm^{-1}; ^1H NMR ($CDCl_3$) δ 7.65–7.22 (m, Ph), 5.26 (s, Cp), 3.21, 3.03 (2 d, ^2J = 2.4 Hz, CH_2); $^{13}C\{^1H\}$ NMR ($CDCl_3$, 220 K) δ 224.2, 214.0, 213.0, 210.0, 208.3, 206.9 (6 s, Fe—CO's), 203.2 (s, Ru—CO), 186.6 (s, =C=), 150.2 (s, =*C*—Ph), 146.2 (s, ipso C of Ph), 128.6, 128.2, 126.8 (3 s, other C's of Ph), 87.2 (s, Cp), 13.3 (s, CH_2); MS (FAB) ^{102}Ru isotope *m/z* 590 (M^+), 562 (M^+ – CO), 534 (M^+ – 2CO), 506 (M^+ – 3CO), 478 (M^+ – 4CO), 450 (M^+ – 5CO), 422 (M^+ – 6CO), 394 (M^+ –

(7) Cotton, F. A.; Wilkinson, G. *Advanced Inorganic Chemistry*, 4th ed.; Wiley: New York, 1980; p 823.
(8) Davidson, J. L. In *Comprehensive Organometallic Chemistry*; Wilkinson, G., Stone, F. G. A., Abel, E. W., Eds.; Pergamon: Oxford, U.K., 1982; Chapter 31.5.
(9) Bennett, M. A.; Bruce, M. I.; Matheson, T. W. In *Comprehensive Organometallic Chemistry*; Wilkinson, G., Stone, F. G. A., Abel, E. W., Eds.; Pergamon: Oxford, U.K., 1982; Chapter 32.4.
(10) Bennett, M. A.; Matheson, T. W. In *Comprehensive Organometallic Chemistry*; Wilkinson, G., Stone, F. G. A., Abel, E. W., Eds.; Pergamon: Oxford, U.K., 1982; Chapter 32.9.
(11) Shriver, D. F.; Drezdzon, M. A. *The Manipulation of Air-Sensitive Compounds*, 2nd ed.; Wiley: New York, 1986.
(12) Shuchart, C. E.; Willis, R. R.; Wojcicki, A. *J. Organomet. Chem.* **1992**, *424*, 185.
(13) Braye, E. H.; Hübel, W. *Inorg. Synth.* **1966**, *8*, 178.
(14) Bruce, M. I.; Jensen, C. M.; Jones, N. L. *Inorg. Synth.* **1989**, *26*, 259.

7CO), 338 (M^+ – 7CO – Fe), 282 (M^+ – 7CO – 2Fe). Anal. Calcd for $C_{21}H_{12}Fe_2O_7Ru$: C, 42.78; H, 2.05. Found: C, 43.54; H, 1.92. Continued elution removed another dark band; cooling the eluent at –23 °C for 24 h afforded black crystals of $(CO)_3FeFe(CO)_3Ru(CO)Cp(\mu_3\text{-}\eta^1\text{:}\eta^2\text{:}\eta^2\text{-}CH{=}C{=}CHPh)$ (**6**; 0.36 g, 15%) while $[Cp(CO)_2Ru]_2$ (0.10 g, 11%), characterized by IR and ^1H NMR spectroscopy,[15] remained in solution. **6**: dec pt 150 °C; IR (Et_2O) ν(CO) 2052 (s), 2019 (vs), 1982 (vs), 1967 (sh), 1917 (w-m, br) cm^{-1}; ^1H NMR ($CDCl_3$) δ 9.16 (d, ^4J < 1 Hz, =CH), 7.46–7.42, 7.36–7.30, 7.24–7.20 (3 m, Ph), 5.14 (s, Cp), 4.76 (s, =C*H*Ph); $^{13}C\{^1H\}$ NMR ($CDCl_3$) δ 212.2 (s, br, Fe—CO's), 203.0 (Ru—CO), 186.2 (s, =C=), 146.2 (s, ipso C of Ph), 128.9 (s, =CH), 128.9, 126.8, 126.7 (3 s, Ph), 87.4 (s, Cp), 36.7 (s, =C*H*Ph); MS (FAB) ^{102}Ru isotope *m/z* 590 (M^+), 562 (M^+ – CO), 534 (M^+ – 2CO), 506 (M^+ – 3CO), 478 (M^+ – 4CO), 450 (M^+ – 5CO), 422 (M^+ – 6CO), 394 (M^+ – 7CO), 338 (M^+ – 7CO – Fe), 282 (M^+ – 7CO – 2Fe). Anal. Calcd for $C_{21}H_{12}Fe_2O_7Ru$: C, 42.78; H, 2.05. Found: C, 42.83; H, 1.79.

Preparation of $(CO)_3RuRu(CO)_3Ru(CO)Cp(\mu_3\text{-}\eta^1\text{:}\eta^2\text{:}\eta^2\text{-}C(Ph){=}C{=}CH_2)$ (7). To a light yellow solution of $Cp(CO)_2RuCH_2C{\equiv}CPh$ (**1**; 1.0 g, 3.0 mmol) in 150 mL of hexane was added $Ru_3(CO)_{12}$ (1.9 g, 3.0 mmol) as a solid. The resulting orange slurry was held at reflux for 7 h, over which time it darkened. At this time, a ^1H NMR spectrum showed that **1** had been essentially consumed. Solvent was removed in vacuo, and the red-brown residue was dissolved in 5 mL of CH_2Cl_2 and treated with an equal volume of alumina (6% H_2O). After solvent had been removed in vacuo, the solid residue was placed on a column of alumina (2.5 × 30 cm) packed in hexane. Elution with 0–5% diethyl ether in hexane gave an extended yellow band that contained unreacted $Ru_3(CO)_{12}$ (0.50 g, identified by IR spectroscopy). The major product was eluted with 15–20% diethyl ether in hexane as a bright yellow-orange band. Several other, small bands were eluted as well but could not be identified. Solvent was evaporated from the collected major band to leave a red solid, **7** (0.20 g, 10% yield): dec pt 85 °C; IR (hexane) ν(CO) 2065 (s), 2033 (vs), 1996 (vs), 1981 (s), 1915 (m) cm^{-1}; ^1H NMR ($CDCl_3$) δ 7.58–7.55, 7.38–7.27 (2 m, Ph), 5.30 (s, Cp), 3.25, 2.85 (2 d, ^2J = 2.3 Hz, CH_2); $^{13}C\{^1H\}$ NMR ($CDCl_3$) δ 202.0 (s, $Ru(CO)_3$), 198.9 (s, CpRu(*C*O)), 179.8 (=C=), 151.5 (s, =*C*Ph), 146.8 (s, ipso C of Ph), 128.4, 128.3, 127.6 (3 s, other C's of Ph), 84.0 (s, Cp), 13.5 (s, CH_2); MS (FAB) ^{102}Ru isotope *m/z* 681 (M^+ – 1), 654 (M^+ – CO), 626 (M^+ – 2CO), 598 (M^+ – 3CO), 570 (M^+ – 4CO), 542 (M^+ – 5CO), 514 (M^+ – 6CO), 486 (M^+ – 7CO). Anal. Calcd for $C_{21}H_{12}O_7Ru_3$: C, 37.12; H, 1.78. Found: C, 37.29; H, 1.80.

Reaction of $(CO)_3Fe(\mu\text{-}\eta^3\text{:}\eta^2\text{-}C(O)C(Ph){=}C{=}CH_2)Ru(CO)Cp$ (2) with PPh_3. A solution of **2** (0.095 g, 0.20 mmol) in hexane (25 mL) was treated with solid PPh_3 (0.052 g, 0.20 mmol), and the resulting solution was stirred at room temperature. Precipitation commenced after ca. 2 h, and the reaction was essentially complete in 16 h. The precipitate was allowed to settle, and the light orange solution was removed via cannula. The solid was washed with hexane (2 × 5 mL) and dried in vacuo to give a red-orange powder of $(PPh_3)(CO)_2Fe(\mu\text{-}\eta^3\text{:}\eta^2\text{-}C(O)C(Ph){=}C{=}CH_2)Ru(CO)Cp$ (**8**; 0.11 g, 77% yield): dec pt 130 °C; IR (CH_2Cl_2) ν(CO) 1992 (vs), 1938 (m), 1919 (m), 1690 (w-m) cm^{-1}; ^1H NMR ($CDCl_3$) δ 7.36–7.23, 7.13–7.01 (2 m, 4Ph), 4.95 (s, Cp), 3.96 (dd, $^2J_{HH}$ = 5.1 Hz, $^4J_{PH}$ = 4.0 Hz, $^1/_2$ of CH_2), 3.64 (d, $^2J_{HH}$ = 5.1 Hz, $^1/_2$ of CH_2); $^{31}P\{^1H\}$ NMR ($CDCl_3$) δ 65.7 (s); $^{13}C\{^1H\}$ NMR ($CDCl_3$) δ 226.3 (d, $^2J_{PC}$ = 17.0 Hz, acyl CO), 219.0 (d, $^2J_{PC}$ = 19.9 Hz, Fe—CO), 209.3 (d, $^2J_{PC}$ = 17.3 Hz, Fe—CO), 203.2 (s, Ru—CO), 188.2 (d, $^2J_{PC}$ = 4.2 Hz, =C=), 134.1 (s, ipso C of Ph), 128.5, 127.4, 126.5 (3 s, Ph of bridging ligand), 133.3 (d, J_{PC} = 10.7 Hz), 132.3 (d, J_{PC} = 1.8 Hz), 129.7 (d, J_{PC} = 1.8 Hz), 128.0 (d, J_{PC} = 10.0 Hz, Ph carbons of PPh_3), 86.2 (s, Cp), 49.8 (d, J_{PC} = 4.3 Hz, =*C*—Ph), 13.8 (s, CH_2); MS (FAB) ^{102}Ru isotope *m/z* 655 (M^+ – 2CO – 1). Anal. Calcd for $C_{36}H_{27}FeO_4PRu$: C, 60.77; H, 3.83. Found C, 60.77; H, 4.15.

(15) Humphries, A. P.; Knox, S. A. R. *J. Chem. Soc., Dalton Trans.* **1975**, 1710.

Reaction of $(CO)_3Fe(\mu\text{-}\eta^3\text{:}\eta^2\text{-}C(O)C(Ph){=}C{=}CH_2)Ru(CO)Cp$ (2) with $Ph_2PCH_2PPh_2$ (dppm). By using a procedure essentially identical with that for the preceding reaction, 0.11 g (71% yield) of red-orange $(\eta^1\text{-dppm})(CO)_2Fe(\mu\text{-}\eta^3\text{:}\eta^2\text{-}C(O)C(Ph){=}C{=}CH_2)Ru(CO)Cp$ (**9**) was obtained from **2** (0.085 g, 0.18 mmol) and dppm (0.069 g, 0.18 mmol): dec pt 142 °C; IR (CH_2Cl_2) ν(CO) 1988 (s), 1942–1910 (w-m, br), 1692 (w) cm^{-1}; ^1H NMR ($CDCl_3$) δ 7.68–7.45 (m, 5Ph), 4.93 (s, Cp), 3.86 (dd, $^2J_{HH}$ = 5.2 Hz, $^4J_{PH}$ = 3.7 Hz, $^1/_2$ of CH_2), 3.56 (dd, $^2J_{HH}$ = 5.2 Hz, $^4J_{PH}$ = 1.4 Hz, $^1/_2$ of CH_2), 3.60–3.41 (m, P—CH_2—P); $^{31}P\{^1H\}$ NMR ($CDCl_3$) δ 60.8 (d, ^2J = 47.0 Hz, coordinated P), –26.0 (d, ^2J = 47.0, dangling P); $^{13}C\{^1H\}$ NMR ($CDCl_3$) δ 228.5 (d, $^2J_{PC}$ = 17.9 Hz, acyl CO), 219.2 (d, $^2J_{PC}$ = 19.4 Hz, Fe—CO), 209.0 (d, $^2J_{PC}$ = 16.8 Hz, Fe—CO's), 203.1 (s, Ru—CO), 190.0 (d, $^2J_{PC}$ = 3.8 Hz, =C=), 139.0 (d, $^1J_{PC}$ = 6.7 Hz, 138.8 (d, $^1J_{PC}$ = 6.7 Hz), 138.5 (d, $^1J_{PC}$ = 5.7 Hz), 138.3 (d, $^1J_{PC}$ = 5.6 Hz) (four different ipso C's of Ph's of dppm), 134.5–126.5 (m, other C's of Ph's), 86.2 (s, Cp), 49.8 (d, $^2J_{PC}$ = 4.4 Hz, =*C*—Ph), 28.1 (dd, $^1J_{PC}$ = 34.4, 23.4 Hz, P—CH_2—P), 13.9 (s, CH_2); Ms (FAB) ^{102}Ru isotope *m/z* 779 (M^+ – 2CO + 1). Anal. Calcd for $C_{43}H_{34}FeO_4P_2Ru$: C, 61.96; H, 4.11. Found: C, 62.56; H, 4.43.

Thermolysis of $(\eta^1\text{-dppm})(CO)_2Fe(\mu\text{-}\eta^3\text{:}\eta^2\text{-}C(O)C(Ph){=}C{=}CH_2)Ru(CO)Cp$ (9). A solution of **9** (0.10 g, 0.12 mmol) in THF (25 mL) was maintained at reflux for 6 h. The resulting deep red solution was freed of solvent, and the residue was dissolved in 1 mL of CH_2Cl_2 and placed on a column of alumina (1 × 20 cm) packed in hexane. Elution with diethyl ether gave an orange band, which after solvent removal afforded $(CO)_2Fe(\mu\text{-}\eta^3\text{:}\eta^2\text{-}C(O)C(Ph){=}C{=}CH_2)(\mu\text{-dppm})RuCp$ (**10**; 0.025 g, 26% yield) as a red solid: ^1H NMR ($CDCl_3$) δ 7.91–7.87, 7.67–7.63, 7.54–7.51, 7.33–7.14, 6.98–6.80 (5 m, 5Ph), 4.40 (s, Cp), 3.71–3.58 (m, P—CH_2—P), 2.80 (ddd, $^2J_{HH}$ = 6.2 Hz, $^4J_{PH}$ = 11.2 Hz, $^2J_{PH}$ = 15.4 Hz, $^1/_2$ of CH_2), 1.98 (dd, $^2J_{HH}$ = 6.2 Hz, $^2J_{PH}$ = 16.8 Hz, $^1/_2$ of CH_2); $^{31}P\{^1H\}$ NMR ($CDCl_3$) δ 61.1 (d, ^2J = 97.4 Hz, Fe—P), 48.8 (d, ^2J = 97.4 Hz, Ru—P); $^{13}C\{^1H\}$ NMR ($CDCl_3$) δ 232.8 (dd, $^2J_{PC}$ = 27.0 Hz, $^4J_{PC}$ = 4.0 Hz, acyl CO), 227.7 (d, $^2J_{PC}$ = 2.5 Hz, Fe—CO), 215.2 (d, $^2J_{PC}$ = 16.9 Hz, Fe—CO), 185.2 (d, $^2J_{PC}$ = 6.8 Hz, =C=), 142.5–126.2 (m, 5Ph), 85.2 (s, Cp), 48.2 (d, $^2J_{PC}$ = 4.2 Hz, =*C*—Ph), 39.9 (t, $^1J_{PC}$ = 17.6 Hz, P—CH_2—P), 14.4 (s, CH_2).

Reaction of $(\eta^1\text{-dppm})(CO)_2Fe(\mu\text{-}\eta^3\text{:}\eta^2\text{-}C(O)C(Ph){=}C{=}CH_2)Ru(CO)Cp$ (9) with Me_3NO. A solution of **9** (0.040 g, 0.048 mmol) in THF (20 mL) was treated with solid Me_3NO (7.2 mg, 0.10 mmol), and the resulting solution was stirred for 18 h at room temperature. Solvent was removed in vacuo, and the residue was dissolved in CH_2Cl_2 (ca. 1 mL) and chromatographed on a column of alumina (1 × 20 cm) packed in hexane. Elution with 20% (v/v) diethyl ether in hexane yielded a small pale orange band of $(CO)_3Fe(\mu\text{-}\eta^3\text{:}\eta^2\text{-}C(O)C(Ph){=}C{=}CH_2)Ru(CO)Cp$ (**2**). Further elution with 25% CH_2Cl_2 in diethyl ether afforded a darker orange band, which was collected and freed of solvent to yield 0.025 g (61%) of $(\eta^1\text{-}Ph_2P(O)CH_2PPh_2)(CO)_2Fe(\mu\text{-}\eta^3\text{:}\eta^2\text{-}C(O)C(Ph){=}C{=}CH_2)Ru(CO)Cp$ (**11**) as a pale orange solid: ^1H NMR ($CDCl_3$) δ 7.80–7.71, 7.47–7.22, 7.08–6.77 (3 m, 5Ph), 4.96 (s, Cp), 4.25–4.00 (m, P—CH_2—P), 3.95 (dd, $^2J_{HH}$ = 5.3 Hz, $^4J_{PH}$ = 4.0 Hz, $^1/_2$ of CH_2) 3.59 (dd, $^2J_{HH}$ = 5.3 Hz, $^4J_{PH}$ = 1.3 Hz, $^1/_2$ of CH_2); $^{31}P\{^1H\}$ NMR ($CDCl_3$) δ 61.9 (d, ^2J = 28.7 Hz, Fe—P), 22.5 (d, ^2J = 28.7 Hz, P=O); $^{13}C\{^1H\}$ NMR ($CDCl_3$) δ 229.2 (d, $^2J_{PC}$ = 17.7 Hz, acyl CO), 220.3 (d, $^2J_{PC}$ = 19.5 Hz, Fe—CO), 208.2 (d, $^2J_{PC}$ = 16.5 Hz, Fe—CO), 202.6 (s, Ru—CO), 189.5 (d, $^2J_{PC}$ = 4.0 Hz, =C=), 133.3–126.5 (m, 5Ph), 86.3 (s, Cp), 51.4 (d, $^2J_{PC}$ = 4.8 Hz, =*C*—Ph), 29.6 (s, P—CH_2—P), 14.3 (s, CH_2).

Reaction of $(CO)_3FeFe(CO)_3Ru(CO)Cp(\mu_3\text{-}\eta^1\text{:}\eta^2\text{:}\eta^2\text{-}C(Ph){=}C{=}CH_2)$ (5) with PPh_3. To a solution of **5** (0.075 g, 0.13 mmol) in hexane (30 mL) was added PPh_3 (0.13 g, 0.50 mmol) as a solid. The resulting brown-green reaction mixture was kept

Table 1. Crystal Data and Data Collection and Refinement of 2, 5, and 6

	2	5	6
	Crystal Data		
molecular formula	$C_{19}H_{12}FeO_5Ru$	$C_{21}H_{12}Fe_2O_7Ru$	$C_{21}H_{12}Fe_2O_7Ru$
fw	477.2	589.1	589.1
cryst syst	monoclinic	monoclinic	monoclinic
space group	$P2_1/c$	$P2_1/c$	$P2_1/c$
a, Å	7.037(5)	8.068(3)	8.999(4)
b, Å	17.20(1)	15.333(4)	12.914(6)
c, Å	29.69(2)	16.849(3)	36.15(1)
β, deg	95.58(5)	95.11(1)	93.46(2)
V, Å	3577(4)	2076.0(4)	4193(3)
Z,	8	4	8
D_{calcd}, g cm^{-3}	1.773	1.885	1.866
F(000), e	1888	1160	2320
μ(Mo Kα), cm^{-1}	16.7	21.2	21.0
cryst size, mm	0.25 × 0.25 × 1.0	0.25 × 0.25 × 0.60	0.30 × 0.30 × 0.70
	Data Collection and Refinement		
temp, °C	21 ± 1	24 ± 1	24 ± 1
radiation		Mo Kα, graphite (λ = 0.710 69)	
scan type	$\omega/2\theta$	$\omega/2\theta$	$\omega/2\theta$
scan speed, deg min^{-1}	1.0–16.5	0.49–4.1	0.82–5.5
scan angle[a]	1.1 + 0.35 tan θ	0.80 + 0.35 tan θ	0.80 + 0.35 tan θ
aperture width, mm	1.1 + tan θ	1.1 + tan θ	1.1 + tan θ
2θ range, deg	6–54	6–56	6–54
rflns, measd	$\pm h,+k,+l$	$\pm h,+k,+l$	$\pm h,+k,+l$
orientatn monitors[b]	2	3	3
intensity monitors[c]	2	3	3
transmissn factors	0.957–0.999	0.915–0.999	0.936–1.000
total no. of rflns measd	8166	5343	9686
no. of rflns with $I > 3\sigma(I)$[d]	5261	3753	6365
data/param ratio	11.2	13.4	11.4
minimized function		$\sum w(\|F_o\| - \|F_c\|)^2$	
w	1	1	1
R[e]	0.065	0.037	0.057
R_w[f]	0.074	0.042	0.075
residuals in final diff map, e Å^{-1}	+1.2, –0.45	+0.66, –1.02	+1.2, –0.73

[a] Extended by 25% on both sides for background measurements. [b] Measured after each 1000 (**2**) or 800 (**5**, **6**) reflections; new orientation matrix if angular change >0.20 (**2**) or >0.11 (**5**, **6**). [c] Measured after each 4000 s. [d] Standard deviation from counting statistics. [e] $R = \sum\|\|F_o\| - \|F_c\|\|/\sum|F_o|$. [f] $R_w = [\sum w(|F_o| - |F_c|)^2/\sum wF_o^2]^{1/2}$.

at reflux for 20 h, over which time the solution turned dark green. Solvent was removed in vacuo, and the residue was dissolved in 2 mL of CH_2Cl_2 and placed on a column of alumina (1 × 20 cm) packed in hexane. Elution with 8–10% (v/v) diethyl ether in hexane developed a green band, which was removed from the column and freed of the solvent to yield $(PPh_3)(CO)_2FeFe(CO)_3Ru(CO)Cp(\mu_3\text{-}\eta^1\text{:}\eta^2\text{:}\eta^2\text{-}C(Ph)=C=CH_2)$ (**12**; 0.045 g, 46%): dec pt 165 °C; IR (Et_2O) ν(CO) 2027 (s), 1969 (s), 1959 (m), 1941 (m), 1938 (sh), 1900 (w-m, br) cm^{-1}; ^{1}H NMR ($CDCl_3$) δ 7.35–7.16, 7.04–6.92 (2 m, 4Ph), 5.23 (s, Cp), 3.21, 3.16 (2 s, CH_2); $^{31}P\{^1H\}$ NMR ($CDCl_3$) δ 71.5 (s); $^{13}C\{^1H\}$ NMR ($CDCl_3$) δ 216.2 (d, $^2J_{PC}$ = 30.9 Hz, $Fe(CO)_2(PPh_3)$), 213.5 (s, $Fe(CO)_3$), 202.5 (s, Ru—CO), 184.0 (s, =C=), 160.3 (s, =*C*—Ph), 143.7 (s, ipso C of Ph of C_3H_2Ph), 134.6–126.9 (m, other C's of 4 Ph), 86.9 (s, Cp), 11.5 (s, CH_2); MS (FAB) ^{102}Ru isotope *m/z* 824 (M^+), 796 ($M^+ - CO$), 768 ($M^+ - 2CO$), 740 ($M^+ - 3CO$), 712 ($M^+ - 4CO$), 684 ($M^+ - 5CO$), 656 ($M^+ - 6CO$). Anal. Calcd for $C_{38}H_{27}Fe_2O_6PRu$: C, 55.43; H, 3.31. Found: C, 56.34; H, 3.13.

Crystallographic Analysis of $(CO)_3Fe(\mu\text{-}\eta^3\text{:}\eta^2\text{-}C(O)C(Ph)=C=CH_2)Ru(CO)Cp$ (2), $(CO)_3FeFe(CO)_3Ru(CO)Cp(\mu_3\text{-}\eta^1\text{:}\eta^2\text{:}\eta^2\text{-}C(Ph)=C=CH_2)$ (5), and $(CO)_3FeFe(CO)_3Ru(CO)Cp(\mu_3\text{-}\eta^1\text{:}\eta^2\text{:}\eta^2\text{-}CH=C=CHPh)$ (6). Crystals of **2** were grown from diethyl ether–hexane at ca. –23 °C and crystals of **5** and **6** from hexane, also at ca. –23 °C. Despite many attempts at crystallization, good-quality crystals of **2** could not be obtained. However, by using the best available crystal, it was possible to determine unambiguously the overall structure of **2**, even if with rather low accuracy.

Lattice constants for **2**, **5**, and **6** were obtained by a least-squares refinement of 25 reflections, accurately centered on an Enraf-Nonius CAD4 diffractometer. A summary of the crystal data and the details of the intensity data collection and refinement are provided in Table 1. No significant change in intensities, due to crystal decay, was observed over the course of all data collections. An empirical absorption correction was applied to observed data based on the ψ scans of four close-to-axial reflections. The heavy-atom positions were determined by the Patterson method for **2** and **5** and by the direct method (MULTAN) for **6**. The whole structures were then determined by conventional Fourier methods. After anisotropic refinement, the calculated idealized positions of hydrogen atoms (C—H = 0.96 Å) all occurred in positive electron density regions. For **2**, no attempt was made to locate the CH_2 hydrogen atoms at C(8). Final full-matrix least-squares refinement of the structures, with the fixed contribution of H atoms ($B = 1.3B_{eq}$Å^2), converged to the R and R_w values given in Table 1. All the non-hydrogen atoms had anisotropic temperature factors. Scattering factors, anomalous dispersion terms, and programs were taken from the Enraf-Nonius SDP library.[16] All computations were carried out on a MicroVAX 2000 computer. Final positional and equivalent thermal parameters are given for **2**, **5**, and **6** in Tables 2–4, respectively. Lists of anisotropic thermal parameters and bond distances and angles for **2**, **5**, and **6** are available as supplementary material.[17]

Results and Discussion

Reactions of $Cp(CO)_2RuCH_2C{\equiv}CPh$ (1) with Iron and Ruthenium Carbonyls. The reaction of **1** with $Fe_2(CO)_9$ is much more complex than the corresponding

(16) B. A. Frenz and Associates, Inc. *Structure Determination Package*; Enraf-Nonius: Delft, Holland, 1985.

(17) See the paragraph at the end of paper regarding supplementary material.

Table 2. Positional and Equivalent Thermal Parameters for 2

	molecule A				molecule B			
atom	*x*	*y*	*z*	*B*,[a] Å²	*x*	*y*	*z*	*B*,[a] Å²
Ru	0.3844(1)	0.23277(6)	0.92296(4)	3.45(2)	0.1151(1)	0.57363(6)	0.82901(4)	3.44(2)
Fe	0.4068(2)	0.1466(1)	0.84573(7)	3.75(4)	0.1138(3)	0.6058(1)	0.91921(7)	3.89(4)
O(1)	0.531(2)	0.0482(7)	0.7745(4)	8.1(3)	−0.014(2)	0.6189(9)	1.0098(4)	9.2(4)
O(2)	0.659(2)	0.0695(6)	0.9145(4)	6.7(3)	−0.111(2)	0.4644(6)	0.9016(4)	7.2(3)
O(3)	0.041(1)	0.0634(7)	0.8514(4)	7.1(3)	0.506(1)	0.5476(7)	0.9476(4)	7.5(3)
O(4)	0.106(1)	0.1250(6)	0.9606(4)	6.5(3)	0.426(1)	0.4539(6)	0.8450(4)	6.3(3)
O(5)	0.736(1)	0.2389(7)	0.8191(4)	6.0(3)	−0.242(1)	0.7012(6)	0.9029(3)	5.4(2)
C(1)	0.478(2)	0.0867(9)	0.8018(5)	5.2(4)	0.049(2)	0.613(1)	0.9757(6)	6.3(4)
C(2)	0.554(2)	0.1028(8)	0.8906(5)	4.7(3)	−0.014(2)	0.5200(8)	0.9060(5)	4.8(3)
C(3)	0.179(2)	0.0950(8)	0.8488(5)	5.0(3)	0.359(2)	0.5692(8)	0.9370(5)	5.2(3)
C(4)	0.207(2)	0.1639(8)	0.9448(5)	4.4(3)	0.305(2)	0.5000(7)	0.8400(5)	4.6(3)
C(5)	0.577(2)	0.2242(8)	0.8272(5)	4.4(3)	−0.080(2)	0.6829(7)	0.9022(4)	3.6(3)
C(6)	0.392(2)	0.2629(8)	0.8197(4)	3.7(3)	0.097(2)	0.7213(7)	0.8902(4)	3.3(3)
C(7)	0.287(2)	0.2513(7)	0.8555(4)	3.5(3)	0.205(1)	0.6687(7)	0.8693(4)	3.4(3)
C(8)	0.137(2)	0.2790(9)	0.8790(4)	4.3(3)	0.344(2)	0.6609(8)	0.8379(5)	4.7(3)
C(9)	0.315(2)	0.2968(7)	0.7752(4)	3.6(3)	0.164(2)	0.7987(7)	0.9077(4)	3.5(3)
C(10)	0.120(2)	0.3090(8)	0.7645(5)	4.3(3)	0.355(2)	0.8215(7)	0.9039(5)	4.6(3)
C(11)	0.061(2)	0.3410(8)	0.7224(6)	5.9(4)	0.418(2)	0.8935(8)	0.9200(6)	6.0(4)
C(12)	0.186(3)	0.3615(9)	0.6927(5)	5.9(4)	0.294(3)	0.9424(8)	0.9391(5)	6.7(5)
C(13)	0.375(3)	0.352(1)	0.7036(6)	6.8(5)	0.110(2)	0.9213(8)	0.9432(5)	5.7(4)
C(14)	0.443(2)	0.3197(9)	0.7443(5)	5.1(4)	0.039(2)	0.8469(8)	0.9269(5)	4.6(3)
C(15)	0.466(2)	0.3435(9)	0.9548(6)	6.4(4)	0.020(2)	0.5330(8)	0.7603(5)	5.2(4)
C(16)	0.468(2)	0.2864(9)	0.9901(5)	5.4(4)	−0.106(2)	0.5019(8)	0.7906(5)	4.9(3)
C(17)	0.609(2)	0.233(1)	0.9806(5)	6.0(4)	−0.199(2)	0.5624(8)	0.8103(5)	4.9(3)
C(18)	0.699(2)	0.2554(9)	0.9398(5)	5.8(4)	−0.140(2)	0.6339(8)	0.7921(5)	4.7(3)
C(19)	0.604(2)	0.325(1)	0.9257(5)	6.3(4)	0.006(2)	0.6140(8)	0.7616(5)	4.6(3)

[a] Anisotropically refined atoms are given in the form of the isotropic equivalent thermal parameter defined as $^4/_3[a^2\beta(1,1) + b^2\beta(2,2) + c^2\beta(3,3) + ab(\cos\gamma)\beta(1,2) + ac(\cos\beta)\beta(1,3) + bc(\cos\alpha)\beta(2,3)]$.

Table 3. Positional and Equivalent Thermal Parameters for 5

atom	*x*	*y*	*z*	*B*,[a] Å²
Ru	0.74106(6)	0.19201(3)	0.12053(2)	3.748(8)
Fe(1)	0.67473(9)	0.03312(4)	0.19069(4)	3.11(1)
Fe(2)	0.84652(9)	0.14347(5)	0.26977(4)	3.25(1)
O(1)	0.7774(6)	−0.1004(3)	0.3068(3)	6.1(1)
O(2)	0.8781(6)	−0.0406(3)	0.0706(3)	6.4(1)
O(3)	0.3667(6)	−0.0595(3)	0.1413(3)	6.6(1)
O(4)	0.9896(7)	0.3134(3)	0.3136(3)	7.6(1)
O(5)	0.8855(6)	0.0609(3)	0.4264(2)	5.6(1)
O(6)	1.1371(6)	0.0587(4)	0.2133(3)	8.5(1)
O(7)	0.4275(6)	0.1161(4)	0.0406(3)	7.7(1)
C(1)	0.7363(7)	−0.0473(3)	0.2621(3)	4.1(1)
C(2)	0.8035(7)	−0.0119(4)	0.1171(3)	4.3(1)
C(3)	0.4838(7)	−0.0210(4)	0.1592(3)	4.1(1)
C(4)	0.9382(8)	0.2466(4)	0.2977(3)	5.0(1)
C(5)	0.8735(7)	0.0949(4)	0.3663(3)	4.1(1)
C(6)	1.0211(7)	0.0906(5)	0.2349(3)	5.0(1)
C(7)	0.5464(8)	0.1366(4)	0.0790(3)	4.9(1)
C(8)	0.5909(8)	0.2765(4)	0.1938(4)	5.1(1)
C(9)	0.6358(6)	0.1982(3)	0.2317(3)	3.52(9)
C(10)	0.5870(6)	0.1203(3)	0.2621(3)	3.05(9)
C(11)	0.4835(6)	0.1170(3)	0.3299(3)	3.40(9)
C(12)	0.4438(8)	0.0395(4)	0.3659(4)	4.9(1)
C(13)	0.3467(8)	0.0386(5)	0.4300(4)	6.0(2)
C(14)	0.2850(8)	0.1143(5)	0.4588(4)	6.3(2)
C(15)	0.3243(9)	0.1917(5)	0.4242(4)	6.3(2)
C(16)	0.4185(7)	0.1938(4)	0.3595(3)	4.9(1)
C(17)	0.778(1)	0.2773(6)	0.0192(4)	8.2(2)
C(18)	0.8867(9)	0.3077(4)	0.0844(4)	5.9(1)
C(19)	1.0017(8)	0.2436(4)	0.1047(4)	5.4(1)
C(20)	0.9693(9)	0.1717(5)	0.0547(4)	7.2(2)
C(21)	0.834(1)	0.1924(6)	0.0018(4)	8.8(2)

[a] Anisotropically refined atoms are given in the form of the isotropic equivalent thermal parameter defined as $^4/_3[a^2\beta(1,1) + b^2\beta(2,2) + c^2\beta(3,3) + ab(\cos\gamma)\beta(1,2) + ac(\cos\beta)\beta(1,3) + bc(\cos\alpha)\beta(2,3)]$.

reactions of $Cp(CO)_2MCH_2C{\equiv}CPh$ (M = Mo, W),[1,6] $Cp(CO)_2FeCH_2C{\equiv}CPh$,[2,3] and $Cp(NO)_2CrCH_2C{\equiv}CPh$.[3] When carried out at room temperature in hexane, it affords several products, the relative amounts of which depend on the stoichiometry of the reactants and on reaction time. Overall, five products have been isolated by employing different conditions for this reaction: $(CO)_3Fe(\mu\text{-}\eta^3{:}\eta^2\text{-}C(O)C(Ph){=}C{=}CH_2)Ru(CO)Cp$ **(2)**, $(CO)_3Fe(\mu_2\text{-}CO)Ru\text{-}Cp(\mu_2\text{-}CO)Fe(CO)_3(\mu_3\text{-}\eta^1\text{-}CCH{=}CHPh)$ **(3)**, $(CO)_3FeRu(CO)CpFe(CO)_3(\mu\text{-}\eta^1{:}\eta^1{:}\eta^3\text{-}CCHCHPh)$ **(4)**, $(CO)_3FeFe(CO)_3Ru(CO)Cp(\mu_3\text{-}\eta^1{:}\eta^2{:}\eta^2\text{-}C(Ph){=}C{=}CH_2)$ **(5)**, and $(CO)_3FeFe(CO)_3Ru(CO)Cp(\mu_3\text{-}\eta^1{:}\eta^2{:}\eta^2\text{-}CH{=}C{=}CHPh)$ **(6)** (cf. eq 3). The formation of a number of products and the problems associated with their separation prompted a systematic study of reaction conditions with a view to simplifying this system and optimizing the yield of each product. Besides being very sensitive to reactant stoichiometry and time, the reaction was found to be strongly dependent on solvent and temperature.

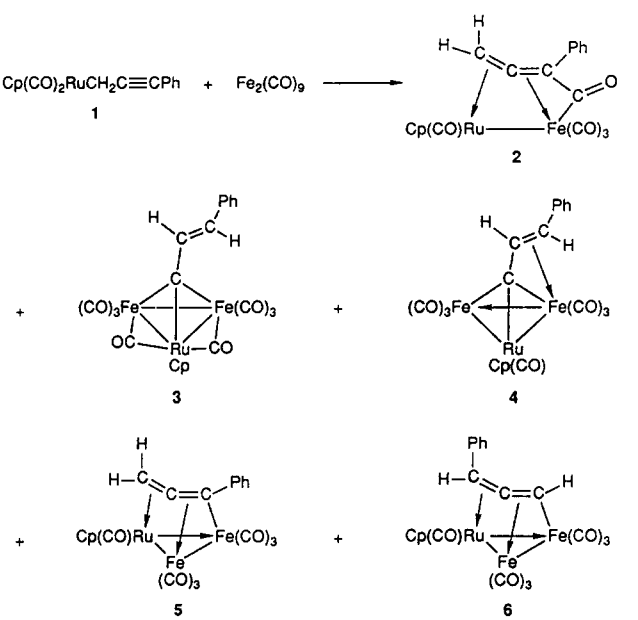

(3)

Table 4. Positional and Equivalent Thermal Parameters for 6

	molecule A				molecule B			
atom	*x*	*y*	*z*	*B*,[a] Å^2	*x*	*y*	*z*	*B*,[a] Å^2
Ru	0.43329(8)	0.72830(6)	0.30273(2)	2.99(1)	0.06566(9)	0.79034(6)	0.05354(2)	3.16(1)
Fe(1)	0.2506(2)	0.8487(1)	0.33945(4)	3.42(3)	0.2863(2)	0.6772(1)	0.08602(5)	4.42(3)
Fe(2)	0.1524(2)	0.7940(1)	0.27557(4)	3.33(3)	0.3276(2)	0.7353(1)	0.02138(5)	4.25(3)
O(1)	0.452(1)	0.8556(8)	0.4057(3)	7.1(3)	0.144(2)	0.6635(9)	0.1151(3)	10.6(4)
O(2)	0.005(1)	0.9452(8)	0.3750(3)	8.0(3)	0.577(1)	0.5975(8)	0.1151(4)	10.0(3)
O(3)	0.347(1)	1.0318(6)	0.2995(3)	5.9(2)	0.186(1)	0.4853(7)	0.0480(3)	6.8(2)
O(4)	−0.0917(9)	0.9391(7)	0.2820(3)	6.3(2)	0.580(1)	0.5975(8)	0.0161(4)	10.6(3)
O(5)	0.278(1)	0.9075(9)	0.2133(3)	8.3(3)	0.155(1)	0.6146(8)	−0.0351(3)	7.7(3)
O(6)	−0.041(1)	0.6441(7)	0.2362(3)	6.7(2)	0.453(2)	0.892(1)	−0.0239(5)	15.7(5)
O(7)	0.3252(9)	0.5951(7)	0.2390(2)	5.2(2)	0.132(1)	0.9392(7)	−0.0073(3)	6.3(2)
C(1)	0.375(1)	0.8537(9)	0.3798(3)	4.6(3)	0.193(2)	0.665(1)	0.1283(3)	5.9(3)
C(2)	0.103(1)	0.9084(9)	0.3613(3)	4.7(3)	0.461(2)	0.626(1)	0.1030(4)	7.1(3)
C(3)	0.306(1)	0.9596(8)	0.3142(3)	4.2(2)	0.224(1)	0.5622(9)	0.0618(4)	4.8(3)
C(4)	0.004(1)	0.8835(8)	0.2789(4)	4.3(2)	0.478(1)	0.653(1)	0.0199(4)	6.8(3)
C(5)	0.233(1)	0.864(1)	0.2388(3)	4.8(3)	0.214(1)	0.661(1)	−0.0131(4)	5.1(3)
C(6)	0.041(1)	0.7014(8)	0.2503(3)	4.2(2)	0.399(1)	0.831(1)	−0.0083(4)	7.2(3)
C(7)	0.342(1)	0.6530(8)	0.2640(3)	3.8(2)	0.127(1)	0.8772(9)	0.0163(3)	4.1(2)
C(8)	0.116(1)	0.7244(8)	0.3221(3)	3.6(2)	0.392(1)	0.8064(8)	0.0667(3)	4.2(2)
C(9)	0.257(1)	0.6969(7)	0.3374(3)	3.3(2)	0.267(1)	0.8278(7)	0.0860(3)	3.6(2)
C(10)	0.357(1)	0.6185(7)	0.3469(3)	3.5(2)	0.161(1)	0.8966(8)	0.0985(3)	3.6(2)
C(11)	0.328(1)	0.5079(7)	0.3381(2)	2.8(2)	0.159(1)	1.0089(7)	0.0911(3)	3.3(2)
C(12)	0.440(1)	0.4371(8)	0.3447(3)	4.1(2)	0.032(1)	1.0662(9)	0.0982(3)	4.8(3)
C(13)	0.418(1)	0.3332(8)	0.3381(3)	5.0(3)	0.027(2)	1.1728(9)	0.0908(3)	5.3(3)
C(14)	0.278(2)	0.2978(8)	0.3246(3)	5.2(3)	0.144(2)	1.2234(9)	0.0784(3)	5.3(3)
C(15)	0.171(1)	0.3694(9)	0.3170(3)	4.5(2)	0.270(1)	1.1681(9)	0.0712(3)	4.7(3)
C(16)	0.190(1)	0.4718(8)	0.3235(3)	4.0(2)	0.2781(1)	1.0619(8)	0.0779(3)	3.9(2)
C(17)	0.664(1)	0.677(1)	0.3006(5)	7.2(4)	−0.167(1)	0.824(2)	0.0555(6)	9.7(5)
C(18)	0.655(1)	0.753(2)	0.3295(4)	10.4(6)	−0.153(1)	0.783(2)	0.0243(5)	9.6(5)
C(19)	0.617(1)	0.847(1)	0.3118(5)	7.1(4)	−0.108(1)	0.693(1)	0.0260(4)	6.9(3)
C(20)	0.604(1)	0.823(1)	0.2755(4)	6.1(3)	−0.100(1)	0.663(1)	0.0638(6)	10.6(5)
C(21)	0.630(1)	0.730(1)	0.2688(4)	7.5(4)	−0.138(1)	0.758(1)	0.0839(3)	9.2(4)

[a] Anisotropically refined atoms are given in the form of the isotropic equivalent thermal parameter defined as $^4/_3[a^2\beta(1,1) + b^2\beta(2,2) + c^2\beta(3,3) + ab(\cos\gamma)\beta(1,2) + ac(\cos\beta)\beta(1,3) + bc(\cos\alpha)\beta(2,3)]$.

The binuclear complex **2** is best prepared, in a 31% isolated yield,[18] by reaction of **1** with 2 equiv of $Fe_2(CO)_9$ in THF at 0 °C. Above this temperature, the higher nuclearity metal complexes form as well. After the reaction at 0 °C has proceeded for 24 h—at which time it is still incomplete—the yield of **2** begins to decrease, owing to the formation of the trinuclear metal clusters.

In diethyl ether at reflux, the foregoing reaction is complete in 20 min, but the yield of **2** significantly decreases. The clusters **3** and **4** also form as isolable products.

The two trinuclear metal μ_3-η^1:η^2:η^2-allenyl products **5** and **6** are best obtained as a readily separable mixture by reaction of **1** with a large excess (6 equiv) of $Fe_2(CO)_9$ in hexane at reflux for 10 min. Under these conditions, $[Cp(CO)_2Ru]_2$ is also produced; however, complexes **2**–**4** are not observed.

Other synthetic approaches to **2** were explored, but with poor results. The reaction of **1** with $Fe_3(CO)_{12}$ in hexane at reflux led to decomposition of the propargyl complex within 3 h. Only small amounts of **2** and **5** were observed in a ^{1}H NMR spectrum of the reaction solution. Photolysis of **1** and $Fe(CO)_5$ in THF for 3 h resulted in the consumption of the propargyl complex and formation of a number of unidentified products, as shown by ^{1}H NMR spectroscopy. Treatment of **1** and $Fe(CO)_5$ in THF with Me_3NO at 0 °C gave virtually no reaction in 3 h, with only a trace of **2** being produced.

Notwithstanding the complexity of the reacting system in eq 3, possible pathways leading to the formation of the various products merit comment. The reaction of **1** with $Fe_2(CO)_9$ to afford **2** may proceed analogously to the reaction of the congeneric propargyl complex $Cp(CO)_2FeCH_2C{\equiv}CPh$ with $Fe_2(CO)_9$ (eq 2);[2,3] suggested pathways for both reactions are shown in Scheme 1. They exhibit some features in common with the mechanism proposed for the [3 + 2] cycloaddition reactions of $L_nMCH_2C{\equiv}CR$.[19] Initially, the propargylic C≡C bonds to a coordinatively unsaturated $Fe(CO)_4$ species to produce a binuclear acetylene complex, which rearranges to a dipolar metal allene complex bearing an $Fe(CO)_3$ group as the negative

Scheme 1

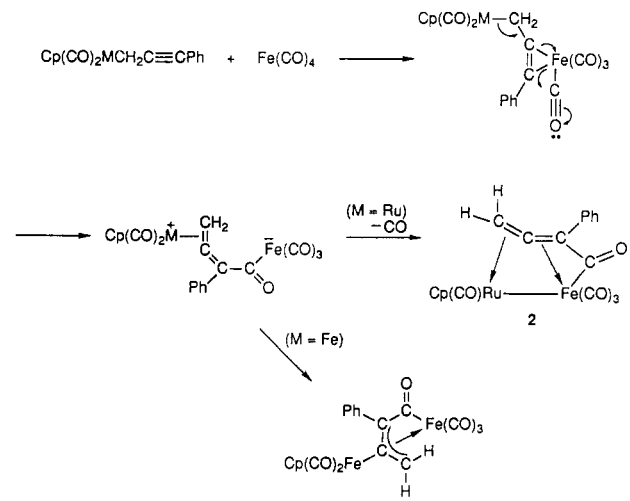

(18) The yield is based on the amount of **1** employed rather than consumed in the reaction, since unreacted **1** decomposes during chromatographic separation/purification.[12]

(19) (a) Rosenblum, M. *Acc. Chem. Res.* **1974**, *7*, 122. (b) Wojcicki, A. In *Fundamental Research in Organometallic Chemistry*; Tsutsui, M., Ishii, Y., Huang, Y., Eds.; Van Nostrand-Reinhold: New York, 1982; pp 569–597. (c) Welker, M. E. *Chem. Rev.* **1992**, *92*, 97.

terminus. This zwitterion then collapses by attack of the negative $Fe(CO)_3$ fragment either at the coordinated allene (for M = Fe) or at the $M(CO)_2Cp$ group with loss of a CO (for M = Ru). The observed selectivity may be due to the relative strength of the incipient Fe—M bond, the susceptibility of $M(CO)_2Cp$ to attack by $Fe(CO)_3^-$, the propensity of $M(CO)_2Cp$ to decarbonylation, or a combination of these factors. Close monitoring of the reaction of **1** with $Fe_2(CO)_9$ at 0 °C by ^1H NMR spectroscopy revealed no observable intermediates during the formation of **2**.

The binuclear complex **2** can be a precursor of the cluster **5** in the general reaction shown in eq 3. It reacts with a 2-fold excess of $Fe_2(CO)_9$ in hexane at reflux to afford the trinuclear Fe_2Ru complexes; for example, after ca. 10 min, **5** (35%), **3** (31%), and unreacted **2** (17%), as well as small amounts of **4**, **6**, and $[Cp(CO)_2Ru]_2$, have been detected by ^1H NMR spectroscopy. Furthermore, keeping a solution of **2** in hexane at reflux for 6 h leads to the formation of equal amounts of **5** and $[Cp(CO)_2Ru]_2$ (eq 4). This reaction apparently proceeds by decomposition of **2** to generate a coordinatively unsaturated mononuclear iron carbonyl fragment, which reacts with **2** to form **5**.

$$2 \xrightarrow{\Delta} 5 + [Cp(CO)_2Ru]_2 \qquad (4)$$

In contrast, the pathways that lead to the formation of the trinuclear clusters **3**, **4**,[20,21] and **6** are not clear. These complexes are formed with accompanying rearrangements of the propargyl or allenyl ligand which involve 1,3- or both 1,2- and 1,3-hydrogen migration from the CH_2 carbon. Such hydrogen shifts had not been previously encountered in the reactions of metal propargyl complexes with metal carbonyls.[22] It is probable that they proceed via metal hydrido intermediates; however, the nature of these processes could not be investigated because of the complexity of the reacting system. Neither **5** nor **6** reacts with excess $Fe_2(CO)_9$ in hexane at reflux, and **3** affords only small amounts of **4**, **5**, and $[Cp(CO)_2Ru]_2$.

A triruthenium cluster, **7**, strictly analogous to **5** results from the reaction of **1** with $Ru_3(CO)_{12}$ in hexane at reflux (eq 5). Other products are formed as well, but in insufficient quantities for characterization.

$Cp(CO)_2RuCH_2C{\equiv}CPh$ + $Ru_3(CO)_{12}$ ⟶

1

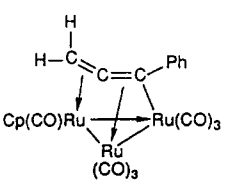

7 (5)

Characterization of Metal μ-Allenylcarbonyl and μ-Allenyl Products. The orange heterobinuclear metal μ-η^3:η^2-allenylcarbonyl complex **2** is stable to air in the solid but decomposes gradually in solution. The Fe_2Ru trinuclear μ_3-η^1:η^2:η^2-allenyl clusters **5** and **6**, respectively, are green-black and black solids that are stable to air. Both are soluble in hydrocarbon, ether, and chlorinated hydrocarbon solvents, with **6** being less soluble than **5** in hydrocarbons. Their solutions decompose upon prolonged storage in air. The red triruthenium μ_3-η^1:η^2:η^2-allenyl complex **7** has stability and solubility properties similar to those of **5** and **6**. Characterization of **2** and **5–7** was accomplished by a combination of elemental analysis, mass spectrometry, and IR and ^1H and ^{13}C NMR spectroscopy (cf. Experimental Section). Unequivocal confirmation of the structures of **2**, **5**, and **6** was obtained by X-ray diffraction analysis. As was stated earlier, the "capped" trinuclear clusters **3** and **4** will be considered elsewhere.[20]

(i) Complex 2. The IR spectrum of **2** in the ν(CO) region shows bands at 2014–1968 cm^{-1} due to terminal CO's and at 1761 cm^{-1} due to a bridging or, possibly, an acyl-type CO. However, η^1-acyl complexes generally absorb at lower wavenumbers, ≤1650 cm^{-1}.[23] In the $^{13}C\{^1H\}$ NMR spectrum, signals are observed at δ 221.7, ca. 210, and 201.5 and are respectively assigned to either a bridging or an acyl CO, Fe-bound CO's, and a Ru-attached CO. The signal at δ ca. 210, which is broad at ambient temperature, separates into three sharp resonances at δ 214.3, 210.6, and 204.7 upon cooling the solution to 220 K, consistent with the number of FeCO's in the molecule. No other $^{13}C\{^1H\}$ NMR signals are affected in appearance by the fluxionality of the iron carbonyl groups.

The resonances of the three carbon atoms of the parent propargyl ligand now occur at δ 46.3, 186.3, and 15.3 and are assigned to C_α, C_β, and C_γ, respectively, of a rearranged, $-C(Ph){=}C{=}CH_2$, allenyl fragment. The assignment of the resonance at δ 15.3 to the CH_2 carbon was confirmed by a 2D $^{13}C\{^1H\}$–^1H correlation NMR spectrum. Further evidence for the sp^2 hybridization at this carbon is provided by the magnitude of the $^1J_{CH}$ coupling constants (162.6, 170.1 Hz) observed in the ^{13}C NMR spectrum.[24] The ^1H NMR spectrum of **2** also shows the CH_2 protons to be inequivalent (δ 4.07, 3.09) and to be unusually strongly coupled ($^2J_{HH}$ = 6.0 Hz) for an sp^2-hybridized carbon atom.

An X-ray analysis of **2** was undertaken, since the foregoing spectroscopic data could not unequivocally resolve the question of the structure of the ligand containing the allenyl fragment $C(Ph){=}C{=}CH_2$ and of the connectivity of this ligand to the two metals. Crystals of **2** contain two crystallographically independent molecules (A and B) that have essentially the same structure, shown in Figure 1. Selected bond distances and angles are given in Table 5.

Molecules of **2** are comprised of an $Fe(CO)_3$ and a Ru(CO)Cp fragment joined by an Fe—Ru single bond that is supported by a bridging $C(O)C(Ph)CCh_2$ ligand. This ligand may be regarded as a resonance hybrid of an allenylcarbonyl (**2A**) and a β-vinylketenyl (**2B**) structure. It is attached to the iron atom through the acyl (or the ketenyl) CO carbon atom (C(5)) as well as through C(6) and C(7) and to the ruthenium atom through the terminal C=C double bond (C(7) and C(8)). The average iron–carbon bond distances are significantly different: Fe–C(5) = 1.92(1) Å, Fe–C(6) = 2.15(1) Å, and Fe–C(7) = 2.00(1)

(20) Complexes **3** and **4** will be considered in another paper together with structurally similar Fe_2Ru "capped" clusters derived from $Cp(CO)_2RuCH{=}C{=}CH_2$ and $Fe_2(CO)_9$. Shuchart, C. E.; Wojcicki, A.; Calligaris, M.; Faleschini, P.; Churchill, M. R.; See, R. F. To be submitted for publication.

(21) Complexes **3** and **4** interconvert to yield a mixture of the two clusters.[20]

(22) However, formation of the tetranuclear Os_3W hydrido cluster has been observed in the reaction of $Cp(CO)_2WCH_2C{\equiv}CCH{=}CH_2$ with $Os_3(CO)_{10}(MeCN)_2$.[4]

(23) Collman, J. P.; Hegedus, L. S.; Norton, J. R.; Finke, R. G. *Principles and Applications of Organotransition Metal Chemistry*, 2nd ed.; University Science Books: Mill Valley, CA, 1987; p 107.

(24) Cooper, J. W. *Spectroscopic Techniques for Organic Chemists*; Wiley-Interscience: New York, 1980; p 87.

Table 5. Selected Bond Distances (Å) and Angles (deg) for 2

	molecule A	molecule B		molecule A	molecule B
Ru–Fe	2.748(2)	2.736(2)	O(5)–C(5)	1.20(2)	1.19(2)
Ru–C(7)	2.08(1)	2.09(1)	C(5)–C(6)	1.46(2)	1.48(2)
Ru–C(8)	2.22(1)	2.20(1)	C(6)–C(7)	1.37(2)	1.37(2)
Fe–C(5)	1.91(1)	1.93(1)	C(6)–C(9)	1.50(2)	1.49(2)
Fe–C(6)	2.14(1)	2.16(1)	C(7)–C(8)	1.40(2)	1.42(2)
Fe–C(7)	2.02(1)	1.99(1)			
Fe–Ru–C(4)	92.4(4)	92.1(4)	C(2)–Fe–C(5)	100.3(6)	100.7(6)
Ru–Fe–C(1)	166.1(4)	163.7(4)	C(3)–Fe–C(5)	157.5(6)	156.2(6)
Ru–Fe–C(2)	71.2(5)	70.2(5)	Fe–C(5)–O(5)	146(1)	146(1)
Ru–Fe–C(3)	95.6(5)	96.8(5)	Fe–C(5)–C(6)	77.9(8)	77.3(7)
Ru–Fe–C(5)	87.3(4)	87.3(4)	O(5)–C(5)–C(6)	135(1)	136(1)
C(1)–Fe–C(2)	96.9(7)	95.5(7)	C(5)–C(6)–C(7)	111(1)	109(1)
C(1)–Fe–C(3)	93.9(7)	94.0(7)	C(5)–C(6)–C(9)	124(1)	124(1)
C(1)–Fe–C(5)	87.9(6)	87.8(7)	C(7)–C(6)–C(9)	125(1)	125(1)
C(2)–Fe–C(3)	101.8(6)	102.7(6)	C(6)–C(7)–C(8)	146(1)	144(1)

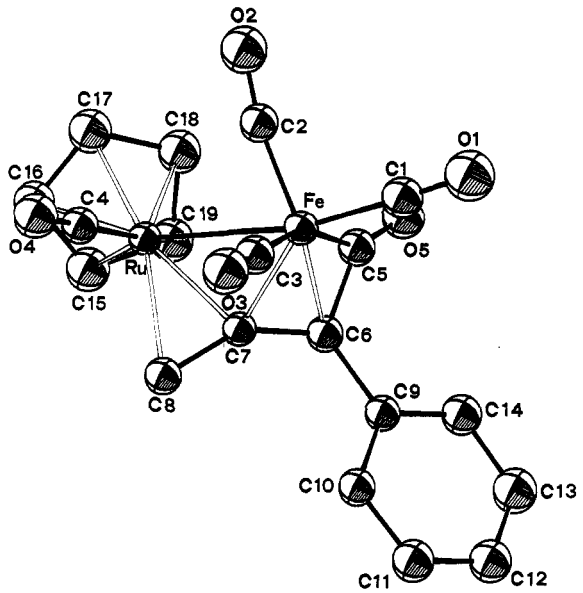

Figure 1. ORTEP plot of **2** showing the atom-numbering scheme. Non-hydrogen atoms are drawn at the 50% probability level. Hydrogen atoms are omitted for clarity.

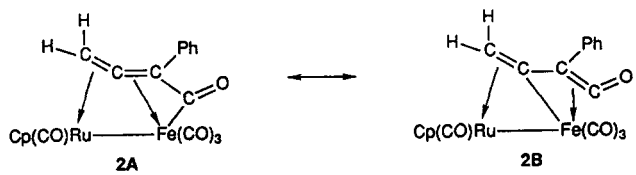

Å. These values are more in line with resonance form **2A** than with **2B**.[25] The average ruthenium–carbon bond distances Ru–C(7) = 2.08(1) Å and Ru–C(8) = 2.21(1) Å are somewhat shorter (0.05–0.06 Å) than the corresponding Ru—C bond lengths reported for the ligated terminal C=C bond in $(CO)_3RuW(CO)_2CpRu(CO)_3(\mu_3\text{-}\eta^1{:}\eta^2{:}\eta^2\text{-}C(Ph)=C=CH_2)$.[1] However, they are consistent with the general trend that the distance M—C_β is shorter than M—C_γ in metal–μ-allenyl complexes.[5b]

The C(5)–C(6) bond distance of 1.48(2) Å (av) is elongated from the 1.42-Å average distance of the RR'C—CO bond in metal C,C-bound ketene complexes.[26] The other C—C bond distances, viz. C(6)–C(7) = 1.37 Å (av) and C(7)–C(8) = 1.41 Å (av), are similar to those found in trinuclear metal $\mu_3\text{-}\eta^1{:}\eta^2{:}\eta^2$-allenyl compounds.[5b] All of these data favor the resonance from **2A** over **2B**. The allenyl C(6)–C(7)–C(8) bond angle of 145(1)° falls in the range reported for the corresponding angle in binuclear and trinuclear μ-allenyl complexes.[5b]

The carbonyl part of the bridging ligand is characterized by a C=O (C(5)–O(5)) bond distance of 1.20(2) Å (av) and an O(5)–C(5)–C(6) bond angle of 136(1)° (av). Whereas the former is compatible with either representation **2A** or **2B**, the latter is suggestive of the resonance form **2B**. Metal C,C-bound ketene complexes show O–C–C bond angles of 135–145°,[26] while metal acyl complexes exhibit the corresponding angles of ca. 120°.[27] However, the magnitude of the O(5)–C(5)–C(6) bond angle in **2** may also be influenced by the bonding requirements of the bridging ligand as a whole, thus resulting in possible distortions at C(5).

To our knowledge, **2** represents the first example of a metal μ-allenylcarbonyl compound. The bonding of the μ-C(O)C(Ph)=C=CH_2 ligand to iron shows close similarities to the bonding of the μ-C(O)C(Ph)=C(Ph) ligand to one ruthenium atom (RuCp) in $Cp(CO)Ru(\mu\text{-}\eta^1{:}\eta^3\text{-}C(Ph)=C(Ph)C(O))(\mu\text{-}CO)RuCp$, which also occurs through three carbon atoms.[28] In fact, the relative values of the Ru—C bond distances in question parallel those of the corresponding Fe—C bond distances in **2**, and the already presented metrical data involving $\mu\text{-}\eta^3{:}\eta^2$-C(O)C(Ph)=C=$CH_2$ are remarkably similar to the corresponding data for $\mu\text{-}\eta^3{:}\eta^2$-C(O)C(Ph)=C(Ph).

(ii) Complexes 5–7. Elemental analyses and FAB mass spectra indicate that **5** and **6** are isomeric Fe_2Ru heptacarbonyl complexes and that **7** is related to them by replacement of the two iron atoms with two ruthenium atoms.

IR and NMR spectroscopic data furnish useful structural information. Whereas the IR spectra of **5** and **6** in the ν(CO) region are very similar, the ^{1}H NMR spectra of the two complexes are substantially different. For **5**, the CH_2 proton signals appear at δ 3.21 and 3.03 with a coupling constant of $^2J_{HH}$ = 2.4 Hz. These chemical shifts are similar to those observed for the series of complexes $(CO)_3FeM(CO)_2CpFe(CO)_3(\mu_3\text{-}\eta^1{:}\eta^2{:}\eta^2\text{-}C(R)=C=CH_2)$ (M = Mo, W).[1] In contrast, **6** shows two equal-intensity,

(25) (a) Hermann, W. A.; Gimeno, J.; Weichmann, J.; Ziegler, M. L.; Balbach, B. *J. Organomet. Chem.* **1981**, *213*, C26. (b) Bkouche-Waksman, I.; Ricci, J. S., Jr.; Koetzle, T. F.; Weichmann, J.; Herrmann, W. A. *Inorg. Chem.* **1985**, *24*, 1492.

(26) Geoffroy, G. L.; Bassner, S. L. *Adv. Organomet. Chem.* **1988**, *28*, 1.

(27) Ginsburg, R. E.; Berg, J. M.; Rothrock, R. K.; Collman, J. P.; Hodgson, K. O.; Dahl, L. F. *J. Am. Chem. Soc.* **1979**, *101*, 7218 and references therein.

(28) Dyke, A. F.; Knox, S. A. R.; Naish, P. J.; Taylor, G. E. *J. Chem. Soc., Dalton Trans.* **1982**, 1297.

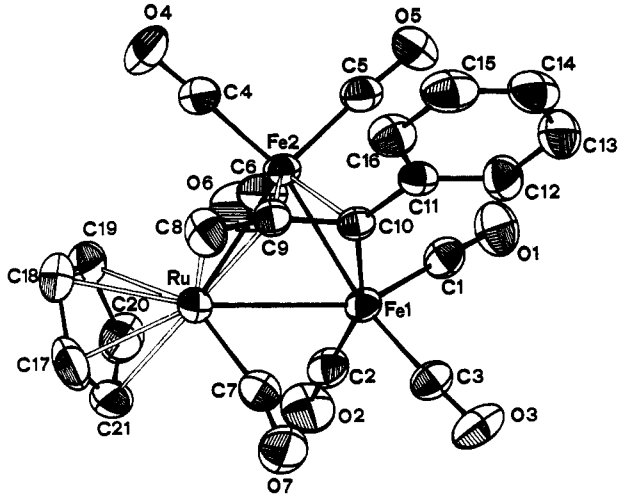

Figure 2. ORTEP plot of **5** showing the atom-numbering scheme. Non-hydrogen atoms are drawn at the 50% probability level. Hydrogen atoms are omitted for clarity.

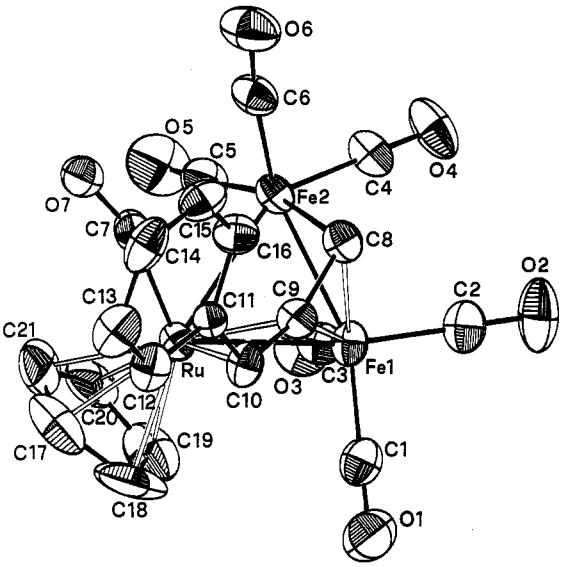

Figure 3. ORTEP plot of **6** showing the atom-numbering scheme. Non-hydrogen atoms are drawn at the 50% probability level. Hydrogen atoms are omitted for clarity.

weakly split (<1 Hz) doublet signals at δ 9.16 and 4.76. With the aid of a 2D $^{13}C\{^1H\}$–^1H correlation NMR spectrum, the resonance at δ 9.16 is assigned to =C*H*Ph and that at δ 4.76 to =CH– of a rearranged, μ_3-η^1:η^2:η^2-CH=C=CHPh, allenyl ligand.

The $^{13}C\{^1H\}$ NMR spectra of **5** and **6** are similar and resemble those reported for related trinuclear metal μ_3-η^1:η^2:η^2-allenyl complexes. Thus, at room temperature, both **5** and **6** show a broad signal at δ 212–211 for fluxional iron carbonyl groups and a singlet at δ ca. 203 for the lone ruthenium carbonyl. The resonances of the allenyl C_α, C_β, and C_γ atoms occur respectively at δ 150.2, 186.6, and 13.3 for **5** and at δ 128.9, 186.2, and 36.7 for **6**. Replacement of hydrogen with a phenyl substituent shifts the resonances of C_α and C_γ to lower field positions by 21–23 ppm.

The spectroscopic data for **7**, which are very similar to those for **5**, support the same type of structure for both complexes. Accordingly, the CH_2 protons of **7** occur at δ 3.25 and 2.85 with a geminal coupling constant of 2.3 Hz. In the ambient-temperature $^{13}C\{^1H\}$ NMR spectrum, one resonance each is noted for the $Ru(CO)_3$ and Ru(CO)Cp carbonyl groups, and the allenyl carbon atoms are seen at δ 179.8 (C_β), 151.5 (C_α), and 13.5 (C_γ).

Unequivocal confirmation of the aforementioned structural features and determination of the μ-allenyl to Fe_2Ru connectivity were achieved by X-ray diffraction analyses of **5** and **6**. The molecular structure of **5** appears in Figure 2, and selected bond distances and angles are provided in Table 6. Crystals of **6** contain two crystallographically independent molecules (A and B) of essentially the same structure. An ORTEP drawing of the molecular structure of **6** is presented in Figure 3, whereas selected bond distances and angles are given in Table 7.

As suggested by the NMR data, the bridging allenyl ligand in **5** and **6** is μ_3-η^1:η^2:η^2-C(Ph)=C=CH_2 and μ_3-η^1:η^2:η^2-CH=C=CHPh, respectively. Apart from this difference, the two structures are remarkably similar and conform to the patterns followed by the previously determined structures of trinuclear metal μ_3-η^1:η^2:η^2-allenyl clusters.[1,4a,29] Accordingly, the carbon–carbon bond distances of the bridging hydrocarbyl ligand (**5**, C(9)–C(10) = 1.371(7) Å, C(8)–C(9) = 1.391(7) Å; **6**, C(8)–C(9) = 1.39(1) Å (av), C(9)–C(10) = 1.40(1) Å (av)), indicative of coordinated C=C double bonds, fall in the range found for other trinuclear metal μ_3-η^1:η^2:η^2-allenyl complexes.[5b] The allenyl ligand is bent, with the C(8)–C(9)–C(10) angle of 148.3(5)° in **5** and 150(1)° (av) in **6** being comparable to that reported (138(2)–152(1)°) for similar complexes. As observed previously,[5b] the M–C_β (i.e. M–C(9)) bond distances are shorter than the corresponding M–C_α and M–C_γ bond distances. Metal–metal interactions involve single Fe–Fe and Fe–Ru bonds.[30]

Table 6. Selected Bond Distances (Å) and Angles (deg) for 5

Ru–Fe(1)	2.7805(8)	Fe(2)–C(9)	1.953(5)
Ru–Fe(2)	2.6868(8)	Fe(2)–C(10)	2.116(5)
Fe(1)–Fe(2)	2.4960(9)	C(8)–C(9)	1.391(7)
Ru–C(8)	2.222(6)	C(9)–C(10)	1.371(7)
Ru–C(9)	2.126(5)	C(10)–C(11)	1.475(7)
Fe(1)–C(10)	1.972(5)		
Fe(1)–Ru–Fe(2)	54.30(2)	C(2)–Fe(1)–C(10)	158.3(2)
Fe(1)–Ru–C(7)	64.7(2)	C(3)–Fe(1)–C(10)	98.6(2)
Fe(2)–Ru–C(7)	114.2(2)	Ru–Fe(2)–Fe(1)	64.77(2)
Ru–Fe(1)–Fe(2)	60.94(2)	Ru–Fe(2)–C(4)	95.2(2)
Ru–Fe(1)–C(1)	148.2(2)	Ru–Fe(2)–C(5)	166.3(2)
Ru–Fe(1)–C(2)	84.2(2)	Ru–Fe(2)–C(6)	90.6(2)
Ru–Fe(1)–C(3)	118.3(2)	Fe(1)–Fe(2)–C(4)	159.3(2)
Ru–Fe(1)–C(10)	76.0(1)	Fe(1)–Fe(2)–C(5)	102.7(2)
Fe(2)–Fe(1)–C(1)	90.0(2)	Fe(1)–Fe(2)–C(6)	86.1(2)
Fe(2)–Fe(1)–C(2)	107.3(2)	C(4)–Fe(2)–C(5)	96.6(3)
Fe(2)–Fe(1)–C(3)	153.6(2)	C(4)–Fe(2)–C(6)	99.7(3)
Fe(2)–Fe(1)–C(10)	55.1(1)	C(5)–Fe(2)–C(6)	94.3(3)
C(1)–Fe(1)–C(2)	93.2(3)	C(8)–C(9)–C(10)	148.3(5)
C(1)–Fe(1)–C(3)	93.5(3)	Fe(1)–C(10)–C(9)	103.4(3)
C(1)–Fe(1)–C(10)	98.8(2)	Fe(1)–C(10)–C(11)	135.1(4)
C(2)–Fe(1)–C(3)	98.7(3)	C(9)–C(10)–C(11)	121.4(4)

A most intriguing feature of each structure is the connectivity of the bridging allenyl ligand to the three metals. In both **5** and **6**, the allenyl is bonded through C_α to one iron, through the internal C=C double bond to the other iron, and through the terminal C=C double bond to ruthenium. This sequence of attachments differs from that in $(CO)_3MW(CO)_2CpM(CO)_3$(μ_3-η^1:η^2:η^2-C(Ph)=

(29) (a) Gervasio, G.; Osella, D.; Valle, M. *Inorg. Chem.* **1976**, *5*, 1221. (b) Nucciarone, D.; MacLaughlin, S. A.; Taylor, N. J.; Carty, A. J. *Organometallics* **1988**, *7*, 106. (c) Suades, J.; Dahan, F.; Mathieu, R. *Organometallics* **1988**, *7*, 47. (d) Shuchart, C. E.; Willis, R. R.; Wojcicki, A.; Rheingold, A. L.; Haggerty, B. S. Manuscript in preparation.

(30) Cotton, F. A.; Walton, R. A. *Multiple Bonds Between Metal Atoms*; Wiley: New York, 1982.

Table 7. Selected Bond Distances (Å) and Angles (deg) for 6

	molecule A	molecule B		molecule A	molecule B
Ru–Fe(1)	2.673(2)	2.679(2)	Fe(1)–C(9)	1.963(9)	1.953(9)
Ru–Fe(2)	2.788(2)	2.783(2)	Fe(2)–C(8)	1.95(1)	1.94(1)
Fe(1)–Fe(2)	2.523(2)	2.503(3)	C(8)–C(9)	1.40(1)	1.38(2)
Ru–C(9)	2.12(1)	2.16(1)	C(9)–C(10)	1.39(1)	1.40(1)
Ru–C(10)	2.27(1)	2.26(1)	C(10)–C(11)	1.48(1)	1.47(1)
Fe(1)–C(8)	2.08(1)	2.06(1)			
Fe(1)–Ru–Fe(2)	54.98(5)	54.53(5)	Ru–Fe(2)–C(6)	116.5(3)	114.9(5)
Fe(1)–Ru–C(7)	115.1(3)	113.6(3)	Ru–Fe(2)–C(8)	75.6(3)	75.0(3)
Fe(2)–Ru–C(7)	62.9(3)	63.6(4)	Fe(1)–Fe(2)–C(4)	88.8(4)	90.2(5)
Ru–Fe(1)–Fe(2)	64.83(5)	64.85(6)	Fe(1)–Fe(2)–C(5)	113.6(4)	111.7(4)
Ru–Fe(1)–C(1)	93.0(4)	92.9(5)	Fe(1)–Fe(2)–C(6)	144.6(4)	148.1(5)
Ru–Fe(1)–C(2)	168.3(4)	165.8(5)	Fe(1)–Fe(2)–C(8)	53.7(3)	53.5(3)
Ru–Fe(1)–C(3)	90.7(4)	92.1(4)	C(4)–Fe(2)–C(5)	93.7(6)	93.6(6)
Fe(2)–Fe(1)–C(1)	157.7(4)	157.8(5)	C(4)–Fe(2)–C(6)	94.0(5)	95.5(7)
Fe(2)–Fe(1)–C(2)	107.5(4)	104.8(5)	C(4)–Fe(2)–C(8)	94.2(5)	97.2(6)
Fe(2)–Fe(1)–C(3)	81.4(4)	81.6(4)	C(5)–Fe(2)–C(6)	101.5(5)	99.3(6)
C(1)–Fe(1)–C(2)	94.1(6)	96.9(7)	C(5)–Fe(2)–C(8)	164.8(5)	161.5(5)
C(1)–Fe(1)–C(3)	101.9(5)	101.1(6)	C(6)–Fe(2)–C(8)	90.9(5)	94.6(6)
C(2)–Fe(1)–C(3)	96.9(5)	96.0(6)	Fe(2)–C(8)–C(9)	105.2(7)	108.3(7)
Ru–Fe(2)–Fe(1)	60.19(5)	60.62(6)	C(8)–C(9)–C(10)	147.7(9)	152(1)
Ru–Fe(2)–C(4)	147.6(4)	148.9(5)	C(9)–C(10)–C(11)	123.1(9)	124.4(9)
Ru–Fe(2)–C(5)	90.8(4)	88.0(4)			

C=CH$_2$) (M = Fe, Ru), where the internal double bond is coordinated to W and the terminal one to Fe or Ru (cf. eq 2).[1] There is no experimental evidence that rearrangement occurs from one type of connectivity to the other with any of these complexes either during or after their preparation. The different connectivities may arise through the trapping by M(CO)$_3$ (M = Fe, Ru) of a different type of binuclear metal μ-η^1:η^2-allenyl precursor. To form **5** and **6**, the precursor would need an uncoordinated terminal C=C double bond, and to form the Fe$_2$W and Ru$_2$W complexes, it would require an uncoordinated internal C=C double bond. However, the reason for this unusual selectivity is not apparent.

Reactions of Metal μ-Allenylcarbonyl and μ-Allenyl Complexes with Phosphines. Substitution reactions of metal carbonyl clusters with phosphines and related ligands are of more than routine interest.[31] They can provide information concerning the presence of labile sites in such polynuclear compounds. Substitution reactions also change electronic and steric balance in the molecule, which may in turn give rise to structural changes. The behavior of complexes **2** and **5** toward phosphines was examined in this general context.

(i) Complex 2. Substitution reactions of **2** with phosphines occur at ambient temperatures. With PPh$_3$, the red-orange, air-stable product (PPh$_3$)(CO)$_2$Fe(μ-η^3:η^2-C(O)C(Ph)=C=CH$_2$)Ru(CO)Cp (**8**) is formed in 77% isolated yield, whereas with dppm, a similar air-stable product, (η^1-dppm)(CO)$_2$Fe(μ-η^3:η^2-C(O)C(Ph)=C=CH$_2$)-Ru(CO)Cp (**9**), is obtained in 71% yield. Both **8** and **9** were characterized as monosubstitution products by elemental analysis and FAB mass spectrometry. The IR ν(C=O) absorptions at 1690 cm^{-1} (for **8**) and 1692 cm^{-1} (for **9**), the CH$_2$ ^{1}H NMR resonances at δ 4.0–3.5, and the ^{13}C{^{1}H} NMR signals at δ ca. 227 (FeC(O)), 190 (=C=), 50 (–*C*(Ph)), and 14 (=CH$_2$) indicate that the μ-allenylcarbonyl ligand has remained intact. The presence of ^{13}C{^{1}H} NMR signals of CO at δ ca. 219 and 209 as doublets

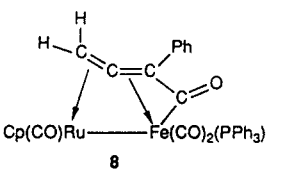

8

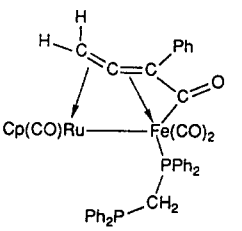

9

(FeCO's) and at δ ca. 203 as a singlet (RuCO) in each spectrum shows that phosphine substitution occurred at the iron center. The ^{31}P{^{1}H} NMR spectrum of **9** shows resonances of ligated (δ 60.8) and free (δ –26.0) phosphine phosphorus atoms,[32] in agreement with a monodentate attachment of dppm.

Attempts were made to force coordination of the pendant phosphine of dppm in **9** by use of photochemical and thermal conditions, and with the aid of Me$_3$NO. Whereas photolysis of **9** resulted in decomposition, thermolysis in THF at reflux yielded a red solid which has been characterized spectroscopically as (CO)$_2$Fe(μ-η^3:η^2-C(O)C-(Ph)=C=CH$_2$)(μ-dppm)RuCp (**10**). Coordination to

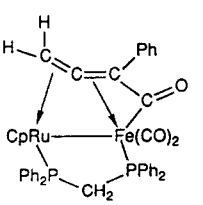

10

metal of both phosphorus atoms of dppm is reflected by the appearance of two signals in the ^{31}P{^{1}H} NMR spectrum at δ 61.1 and 48.8 with a large coupling constant, $^2J_{PP}$, of 97.4 Hz. That dppm bonds in a bridging (to Fe and Ru) rather than chelating (to Fe only) fashion is evidenced by the presence of two FeCO ^{13}C{^{1}H} NMR signals at δ 227.7 and 215.2 and by the notable absence of a resonance due

(31) Darensbourg, D. J. In *The Chemistry of Metal Cluster Complexes*; Shriver, D. F., Kaesz, H. D., Adams, R. D., Eds.; VCH: New York, 1990; Chapter 4.

(32) Pregosin, P. S.; Kunz, R. W. *Phosphorus-31 and Carbon-13 NMR of Transition-Metal Complexes*; Springer-Verlag: New York, 1979.

to RuCO. Furthermore, in the ^1H NMR spectrum, the signal of η^5-C_5H_5 occurs at δ 4.40; this chemical shift may be compared to that farther upfield, at δ 4.96–4.93, for complexes **8**, **9**, and **11**, in which the ruthenium atom is bonded to CO rather than a phosphine phosphorus. There is also a substantial upfield shift (>1 ppm) of the proton resonances of CH_2, which are now more strongly coupled to one (J_{PH} = 16.8 Hz) or both (J_{PH} = 11.2, 15.4 Hz) phosphorus nuclei.

Interestingly, the two FeCO signals, both of which display coupling constants, $^2J_{PC}$, of 16.5–19.9 Hz for complexes **8**, **9**, and **11**, show $^2J_{PC}$ values of 16.9 and only 2.5 Hz for **10**. The value of $^2J_{PC}$ for the μ-allenylcarbonyl CO resonance, which is in the narrow range of 17.0–17.9 Hz for **8**, **9**, and **11**, increases to 27.0 Hz for **10**. These data suggest that one of the FeCO's and the μ-allenylcarbonyl CO assume different orientations with respect to the Fe-bonded phosphrous upon disubstitution. It would appear that the relative positions of the phosphorus atom and the acyl CO are "more trans" in **10** than in the other complexes, probably to enable dppm to bridge across the Fe—Ru bond.

Reaction of **9** with Me_3NO at room temperature resulted in attack of the amine *N*-oxide at the free phosphine phosphorus rather than at the CO (which would have formed CO_2[33]). The product (η^1-$Ph_2P(O)CH_2PPh_2$)-$(CO)_2Fe(\mu\text{-}\eta^3{:}\eta^2\text{-}C(O)C(Ph){=}C{=}CH_2)Ru(CO)Cp$ (**11**), a

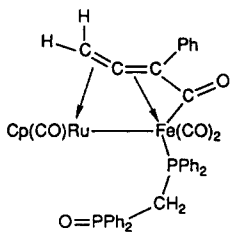

11

pale orange solid, exhibits ^1H and $^{13}C\{^1H\}$ NMR spectra that are very similar to those of **9**. However, the $^{31}P\{^1H\}$ NMR spectrum shows two doublets ($^2J_{PP}$ = 28.7 Hz) at δ 61.9 and 22.5, with the higher field signal, assigned to uncoordinated phosphorus (now P=O), being shifted more than 48 ppm downfield compared to its position for **9**.

(II) Complex 5. At room temperature, no reaction was observed between **5** and excess PPh_3 in hexane solution over several hours. However, when the temperature was increased to ca. 65 °C, replacement of one CO with PPh_3 occurs to yield a dark green solid, **12**. The product was characterized as a monosubstitution derivative of **5** by elemental analysis and FAB mass spectrometry, and the IR and NMR spectra confirm that the gross structure of complex **5** has been retained in **12**. The presence of three $^{13}C\{^1H\}$ NMR signals of CO as a doublet ($^2J_{PC}$ = 30.9 Hz) at δ 216.2 and singlets at δ 213.5 and 202.5 indicates that substitution occurred at one of the iron atoms (**12A** or **12B**). Although an unequivocal structure assignment to

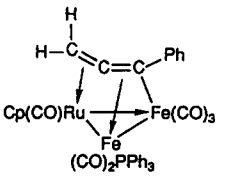

12A

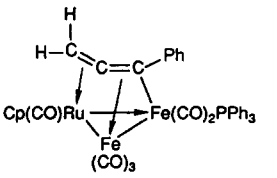

12B

the product cannot be made, **12B** is favored from the ^{13}C NMR data. This is because the chemical shift of =*C*Ph is more affected by PPh_3 substitution ($\Delta\delta$ = 10 ppm) than is the chemical shift of =C= ($\Delta\delta$ = 3 ppm) or $=CH_2$ ($\Delta\delta$ = 2 ppm). Surprisingly, none of the signals of the allenyl carbon atoms of **12** show coupling to phosphorus.

Conclusions

Reaction of $Cp(CO)_2RuCH_2C{\equiv}CPh$ (**1**) with $Fe_2(CO)_9$ is considerably less selective than the previously studied corresponding reactions of related molybdenum, tungsten, iron, and chromium propargyl complexes. When carried out at the lower temperatures in THF, it affords a novel bridging-allenylcarbonyl product, $(CO)_3Fe(\mu\text{-}\eta^3{:}\eta^2\text{-}C(O)C(Ph){=}C{=}CH_2)Ru(CO)Cp$ (**2**). At higher temperatures in various solvents, the trinuclear Fe_2Ru "capped" clusters $(CO)_3Fe(\mu_2\text{-}CO)RuCp(\mu_2\text{-}CO)Fe(CO)_3(\mu_3\text{-}\eta^1\text{-}CCH{=}CHPh)$ (**3**) and $(CO)_3FeRu(CO)CpFe(CO)_3(\mu\text{-}\eta^1{:}\eta^1{:}\eta^3\text{-}CCHCHPh)$ (**4**), as well as the bridging-allenyl clusters $(CO)_3FeFe(CO)_3Ru(CO)Cp(\mu_3\text{-}\eta^1{:}\eta^2{:}\eta^2\text{-}C(Ph){=}C{=}CH_2)$ (**5**) and $(CO)_3FeFe(CO)_3Ru(CO)Cp(\mu_3\text{-}\eta^1{:}\eta^2{:}\eta^2\text{-}CH{=}C{=}CHPh)$ (**6**), are formed, often rather nonselectively. Complex **5** arises, at least in part, by decomposition or reaction with $Fe_2(CO)_9$ of the binuclear complex **2**. However, pathways that lead to the formation of **3**, **4**, and **6** are not readily apparent. They involve 1,3- or both 1,3- and 1,2-hydrogen migration from the CH_2 carbon atom within the C_3H_2Ph ligand and implicate metal μ-hydrido intermediates. Phosphines (PPh_3, dppm) replace an iron-bonded CO in **2** and **5** to give monosubstitution products. Under forcing conditions, the dppm-containing monosubstitution product (η^1-dppm)$(CO)_2Fe(\mu\text{-}\eta^3{:}\eta^2\text{-}C(O)C(Ph){=}C{=}CH_2)Ru(CO)Cp$ (**9**) affords a disubstitution derivative in which dppm bridges across the Fe—Ru bond.

Acknowledgment. We gratefully acknowledge financial support of this investigation by the National Science Foundation, The Ohio State University, and Ministero Pubblica Istruzione (Rome). Mass spectra were obtained at The Ohio State University Chemical Instrument Center (funded in part by National Science Foundation Grant 79-10019). We thank Johnson Matthey Aesar/Alfa for a loan of ruthenium trichloride.

Supplementary Material Available: Tables of anisotropic thermal parameters and of bond distances and angles for complexes **2**, **5**, and **6** (14 pages). Ordering information is given on any current masthead page.

OM9400154

(33) (a) Albers, M. O.; Coville, N. J. *Coord. Chem. Rev.* **1984**, *53*, 227. (b) Luh, T.-Y. *Coord. Chem. Rev.* **1984**, *60*, 255.